26/July/2007, ISSP International Workshop:
Foundations and Applications of the Density Functional Theory

Large scale electronic structure calculation theory and its application

Takeo FUJIWARA
Center for Research and Development of Higher Education, The University of Tokyo
(former at Department of Applied Physics, UT)

Large-scale electronic-structure calculations

Why is it difficult for large systems?

Because electronic wavefunctions are not localized and the CPU resorce should be proportional to N^3!

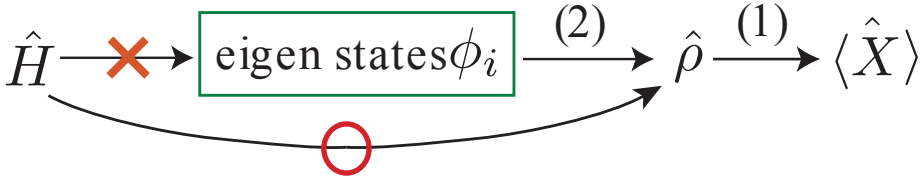

Can we get the density matrix without a knowledge on eigenstates?

Yes, we can get ρ without ϕ.

Calculating a physical quantity $\langle X \rangle$

$$\langle \hat{X} \rangle = \sum_{i}^{\mathrm{occ.}} \langle \phi_i | \hat{X} | \phi_i \rangle = \mathrm{Tr}[\hat{\rho}\hat{\mathrm{X}}] \qquad (1)$$

$$\hat{\rho} \equiv \sum_{i}^{\mathrm{occ}} |\phi_i\rangle\langle\phi_i| \qquad (2)$$

: (one-body) density matrix

Wannier representation.
Hoshi and Fujiwara
J. Phys. Soc. Jpn **69**, 3773 (2000)

Order-N
Hoshi and Fujiwara
J. Phys. Soc. Jpn **72**, 2880 (2003)

Krylov(Subspace Diagonalization)
Takayama, Hoshi and Fujiwara
J. Phys. Soc. Jpn **73**, 1519 (2004)

Nano-scale cleavage in Si
Hoshi, Iguchi, Fujiwara
Phys. Rev. B**72**, 075323 (2005)

Krylov (Shifted COCG)
Takayama, Hoshi and Fujiwara
Phys. Rev. B**73**, 165108 (2006)

Hybrid Method
Hoshi and Fujiwara
J. Phys. Cond. Mat. **18**, 10787 (2006)

Our Large-scale Electronic Structure Calculations

Usually
hybrid method with
quantum mechanical MD *(in small region)*
and
classical mechanical MD *(in larger region)*

Our method
hybrid method with
different kinds of quantum mechanical MDs *(over whole region)*

- *nonlinearity due to shape, force, inhomogenious contact, wavefunctions*
- *non-equilibrium, transient process*

Wannier state method without using eigen states

$$H_{\rm eff}\psi_i = \sum_{j=1}^{\rm occ.} \varepsilon_{ij}\psi_j$$

$$\psi_j = \sum_{k}^{\rm occ.} U_{jk}\psi_k^{\rm (eig)}$$

$$\langle \hat{X} \rangle \equiv \sum_{k}^{\rm occ} \langle \psi_k^{\rm (eig)} | \hat{X} | \psi_k^{\rm (eig)} \rangle = \sum_{j}^{\rm occ} \langle \psi_j | \hat{X} | \psi_j \rangle$$

⟶"generalized Wannier states",
"ab initio bonding orbitals"

Many ab initio applications ⟶ Exact, but not order-N

(1) $$|\phi_j\rangle \approx C^{(0)}|{\rm b}_j\rangle + \sum_{i(\neq j)} C^{(\nu(i))}|{\rm a}_i\rangle. \qquad \frac{C^{(\nu)}}{C^{(0)}} = \frac{\langle a^{(\nu)}|H|b_k\rangle}{\varepsilon_{\rm b} - \varepsilon_{\rm a}}.$$

(2) $$H_{\rm WS}^{(k)}\psi_k = \varepsilon_{kk}\psi_k, \qquad H_{\rm WS}^{(k)} = H - \bar{\rho}_k\Omega - \Omega\bar{\rho}_k$$

$$\bar{\rho}_k = \rho - |\psi_k\rangle\langle\psi_k| = \sum_{j\neq k}^{N} |\psi_j\rangle\langle\psi_j|$$

$$\Omega = H - \mu \quad (\mu > \varepsilon_N)$$

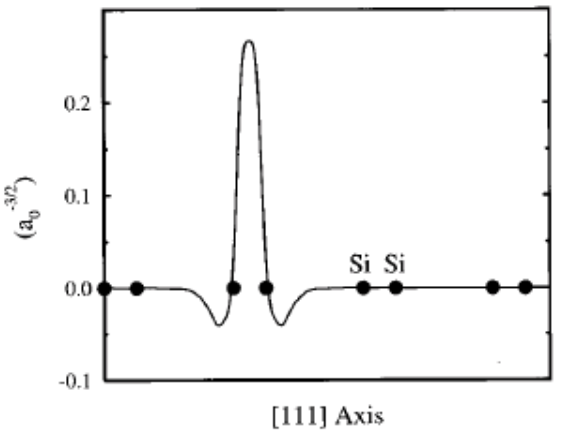

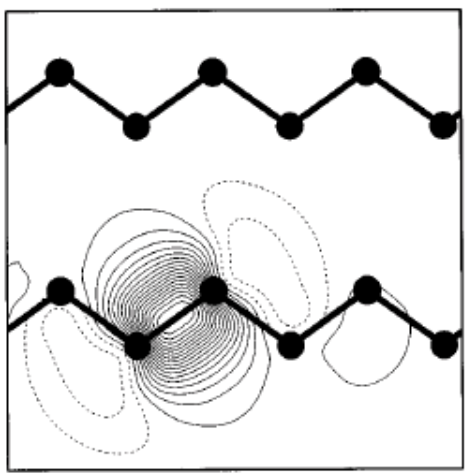

ab initio wfn. in Si crystal
(Marzari & Vanderbilt '97)

Krylov Subspace

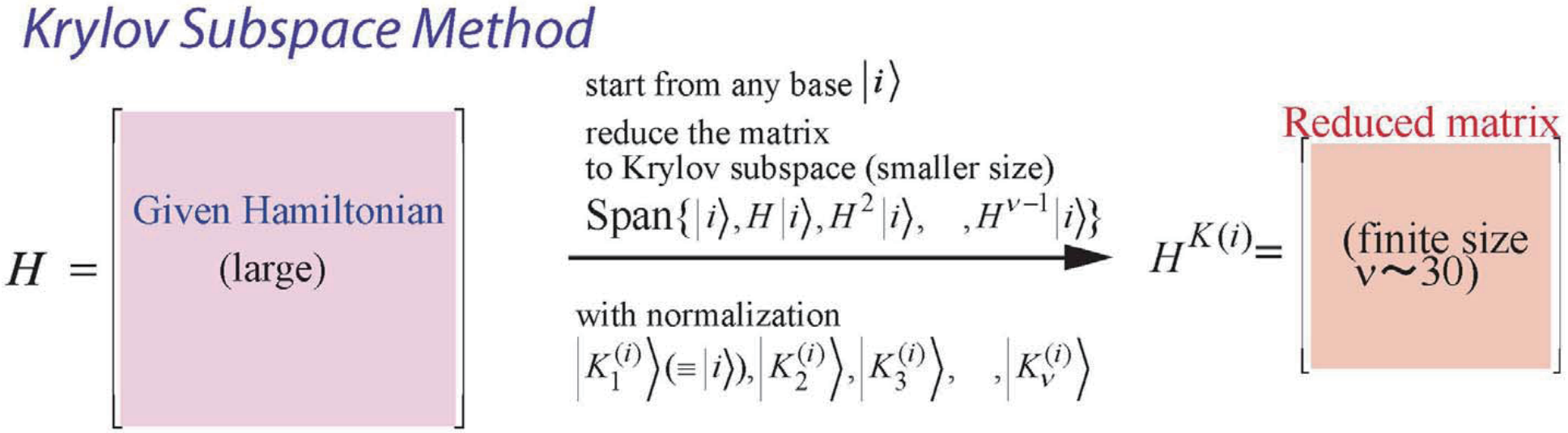

(1) Subspace diagonalization method

(2) Shifted COCG method

Subspace Diagonalization

Takayama, Hoshi and Fujiwara
J. Phys. Soc. Jpn 73, 1519 (2004)

Diagonalize $H^{K(i)}$: $H^{K(i)}\left|w_\alpha\right\rangle = \varepsilon_\alpha \left|w_\alpha\right\rangle$

Density matrix operator: $\hat{\rho}^{K(i)} \equiv \sum_{\alpha}^{\nu} \left|w_\alpha\right\rangle\left\langle w_\alpha\right| f\left(\frac{\varepsilon_\alpha - \mu}{kT}\right)$,

The replacement of the density matrix:

$$\left\langle i\right|\hat{\rho}\left|j\right\rangle \Rightarrow \left\langle i\right|\hat{\rho}^{K(i)}\left|j\right\rangle$$

$$\left\langle i\right|\hat{\rho}^{K(i)}\left|j\right\rangle = \sum_{n}^{\nu}\left\langle i\right|\hat{\rho}^{K(i)}\left|K_n^{(i)}\right\rangle\left\langle K_n^{(i)}\right|\left.j\right\rangle$$

$\left|i\right\rangle$:an element of the KS

$\left|j\right\rangle$:not necessarily in the KS

The convergence of this summation validate the present method.

The advantages of using eigenstates of $H^{K(i)}$ are

- exact calc. is available within reduced Hilbert space
- energy integration

→ reduced matrix size ν

Error can be monitored.

$$\left\langle i\right|r_v^{(j)}\left\rangle = \left\langle i\right|I - (z - H)G_v^{(i)}(z)\left|j\right\rangle$$

Shifted COCG Method and Density Matrix

Takayama, Hoshi and Fujiwara: Phys. Rev. B**73**, 165108 (2006)

$$(z-H)|x_n^{(j)}\rangle = |j\rangle \qquad (z_{ref}+\sigma-H)|x_n^{\sigma j}(z_{ref}+\sigma)\rangle = |j\rangle$$

Green's Function

$$G_{ij}(z_k) \equiv \langle i|x^{(j)}(z_k)\rangle = \langle i|(z_k - H)^{-1}|j\rangle$$

$$\rho_{ij} = -\frac{1}{\pi}\int_{-\infty}^{\infty} \mathrm{Im}G_{ij}(z) f\left(\frac{\varepsilon-\mu}{k_B T}\right) \mathrm{d}\varepsilon$$

Krylov subspace by shifted z is identical to the original subspace.

---

vector–matrix product:*N* times/iteration

Conjugate Orthogonal CG method (COCG)

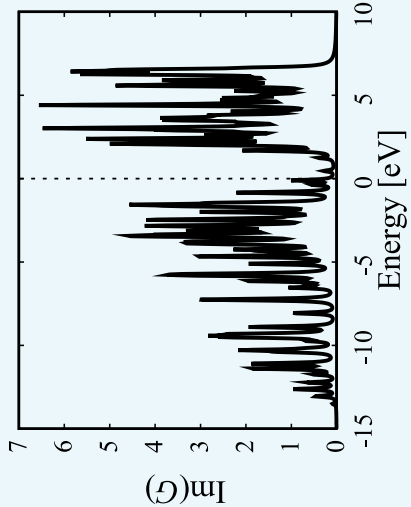

$(z_N - H)\left|x_n^{(j)}(z_N)\right\rangle = |j\rangle$

$(z_3 - H)\left|x_n^{(j)}(z_3)\right\rangle = |j\rangle$

$(z_2 - H)\left|x_n^{(j)}(z_2)\right\rangle = |j\rangle$

$(z_1 - H)\left|x_n^{(j)}(z_1)\right\rangle = |j\rangle$

vector–matrix product:Once /iteration

shifted COCG method

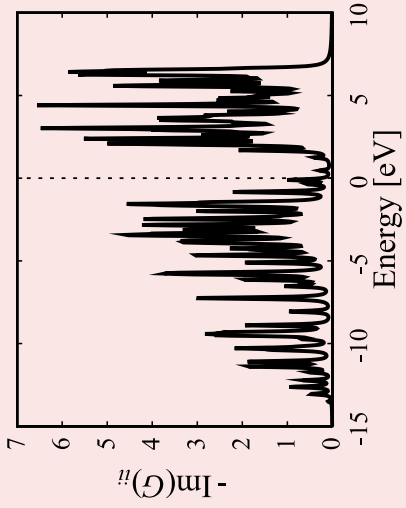

$(z_{\mathrm{ref}} + \sigma_N - H)\left|x_n^{\sigma(j)}(z_{\mathrm{ref}} + \sigma_N)\right\rangle = |j\rangle$

$(z_{\mathrm{ref}} - H)\left|x_n^{(j)}(z_{\mathrm{ref}})\right\rangle = |j\rangle$

$(z_{\mathrm{ref}} + \sigma_2 - H)\left|x_n^{\sigma(j)}(z_{\mathrm{ref}} + \sigma_2)\right\rangle = |j\rangle$

$(z_{\mathrm{ref}} + \sigma_1 - H)\left|x_n^{\sigma(j)}(z_{\mathrm{ref}} + \sigma_1)\right\rangle = |j\rangle$

$La_{3/2}Sr_{1/2}NiO_3$ Application to Many-Body Problem

Stripe order of charge and spin

S.Yamamoto and T.Fujiwara, unpublished

$$H = \sum_{i,j,\alpha,\beta,\sigma} t_{i\alpha j\beta} c^{\dagger}_{i\alpha\sigma} c_{j\beta\sigma} + \sum_{i,\alpha,\sigma} \varepsilon_{i\alpha} c^{\dagger}_{i\alpha\sigma} c_{i\alpha\sigma} + \frac{1}{2} \sum_{i,\alpha,\beta,\gamma,\delta,\sigma,\sigma'} U_{\alpha\beta\gamma\delta} c^{\dagger}_{i\alpha\sigma} c^{\dagger}_{i\beta\sigma'} c_{i\delta\sigma'} c_{i\gamma\sigma} + \frac{V}{2} \sum_{\langle i,j\rangle,\alpha,\beta,\sigma,\sigma'} c^{\dagger}_{i\alpha\sigma} c_{i\alpha\sigma} c^{\dagger}_{j\beta\sigma'} c_{j\beta\sigma'}$$

State A = ground state at V=0eV

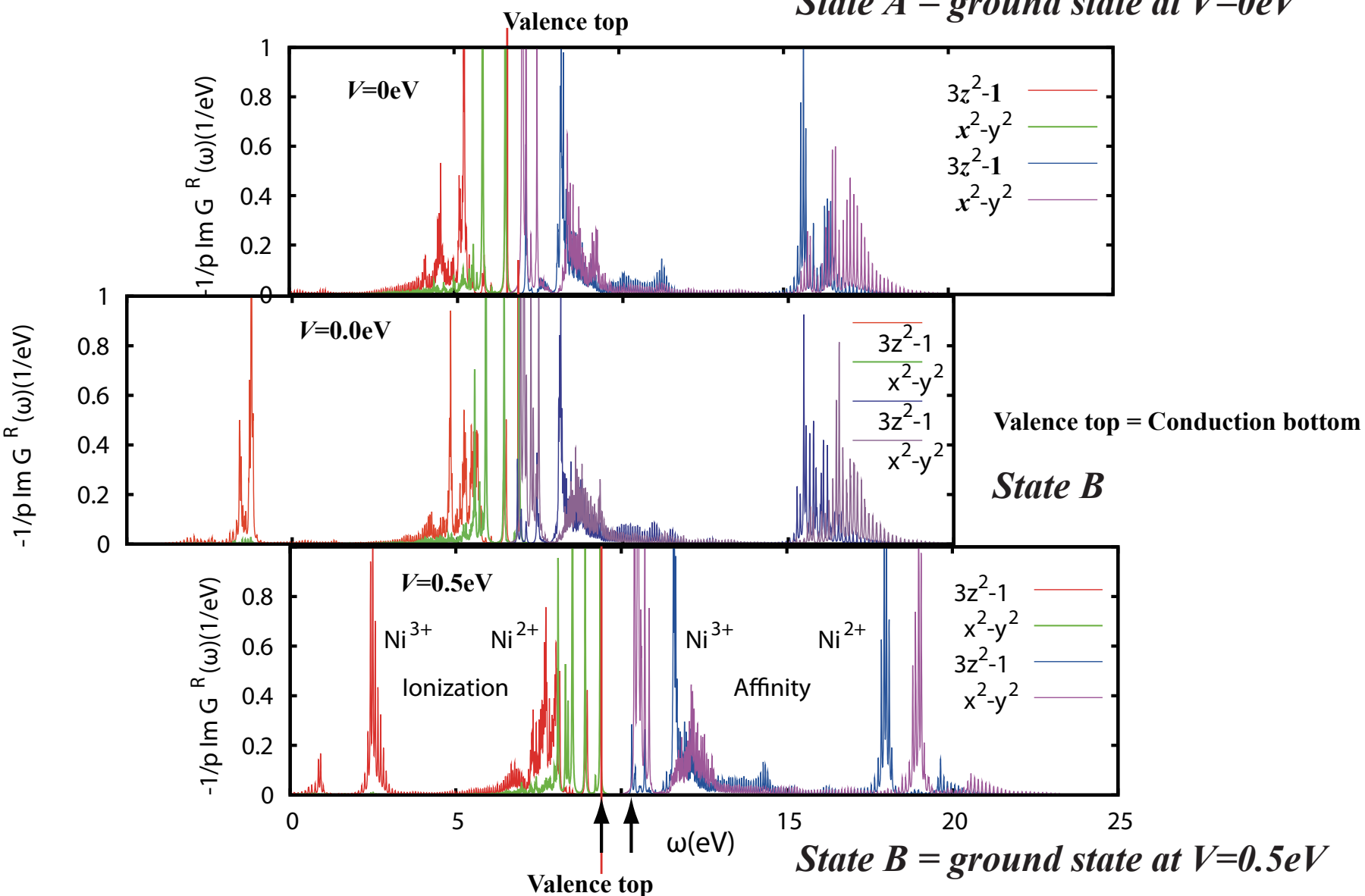

State B = ground state at V=0.5eV

Hybrid Method

$$\rho = \rho_A + \rho_B \qquad \rho_A \rho_B = 0$$

$$H^{(A)} = H + 2\eta\rho_B - (H\rho_B + \rho_B H)$$
$$\cong H + 2(\eta - \varepsilon_B)\rho_B$$

$$H^{(A)}\rho_A - \rho_A H^{(A)} = 0$$

Division of the Hilbert space (not division of real space)

Large-scale Electronic Structure Calculation

10^7 atoms !!
~$(70\ \mathrm{nm})^3$ system !!

Density Matrix Formalism

Wannier state representation
Krylov subspace diagonalizatiopn
shifted COCG method
Hybrid method and parallelization

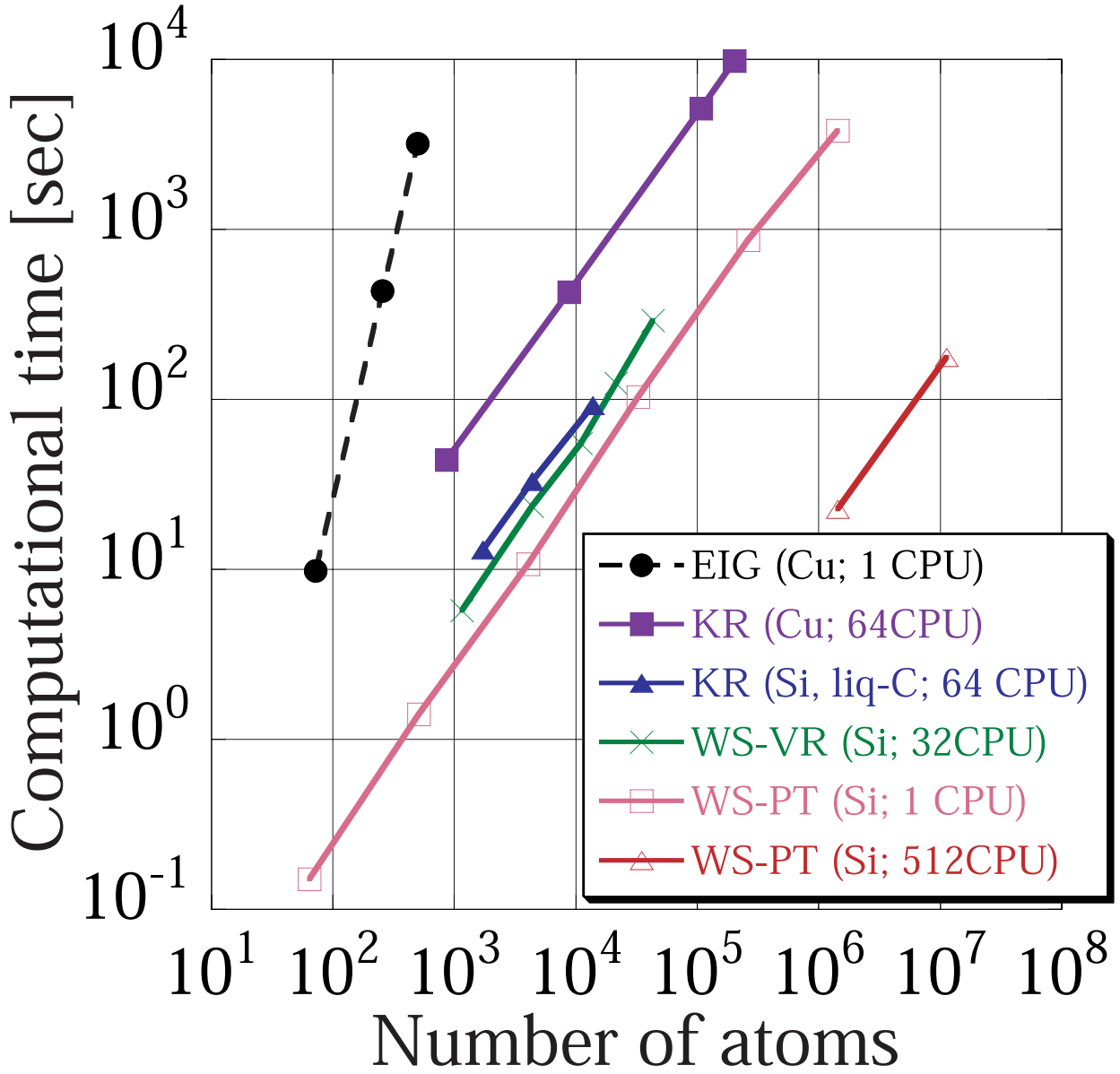

Applications

Fracture Propagation in Si Crystals
Growth Mechanism of Carbon Nanotube
Gold Helical Multishell Nanowire

Dynamical Brittle Fracture Propagation
J. Phys. Soc. Jpn **72**, 2429 (2003)
Nano-scale cleavage in Si
Phys. Rev. B**72**, 075323 (2005)

METHODOLOGY
Wannier function method
J. Phys. Soc. Jpn **69**, 3773 (2000)
Krylov Subspace Diagonalization
J. Phys. Soc. Jpn **73**, 1519 (2004)

Fracture simulation (1)

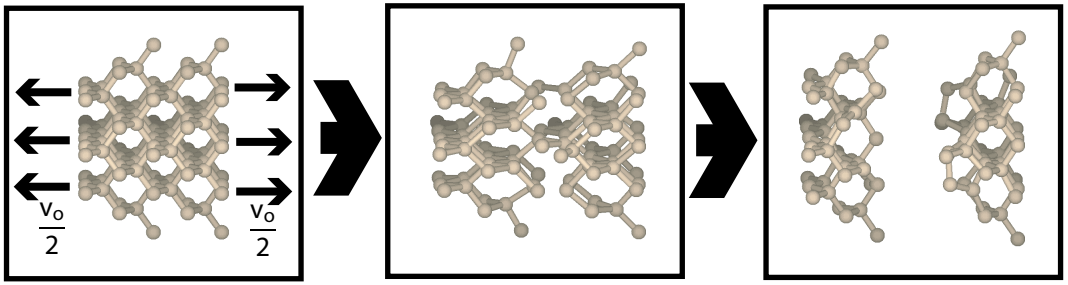

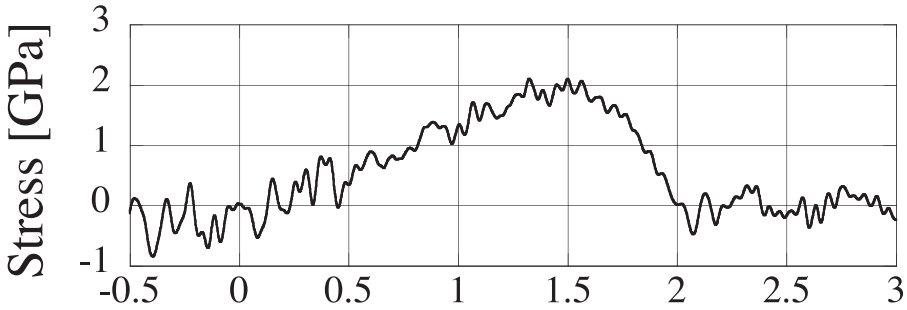

[001] external load,
isolated cluster with 91 atoms,
an initial "defect" bond,
exact diagonalization
$v_0 = 0.1$[K m/s]
Tight-binding, T = 300 K

Reasonable crack-propagation speed

$v_{crack} \approx 2$ [km/s]

(Exp. $v_{crack} \lesssim 3.8$ [km/s])

Fracture begins as level crossings of several "defect" states.

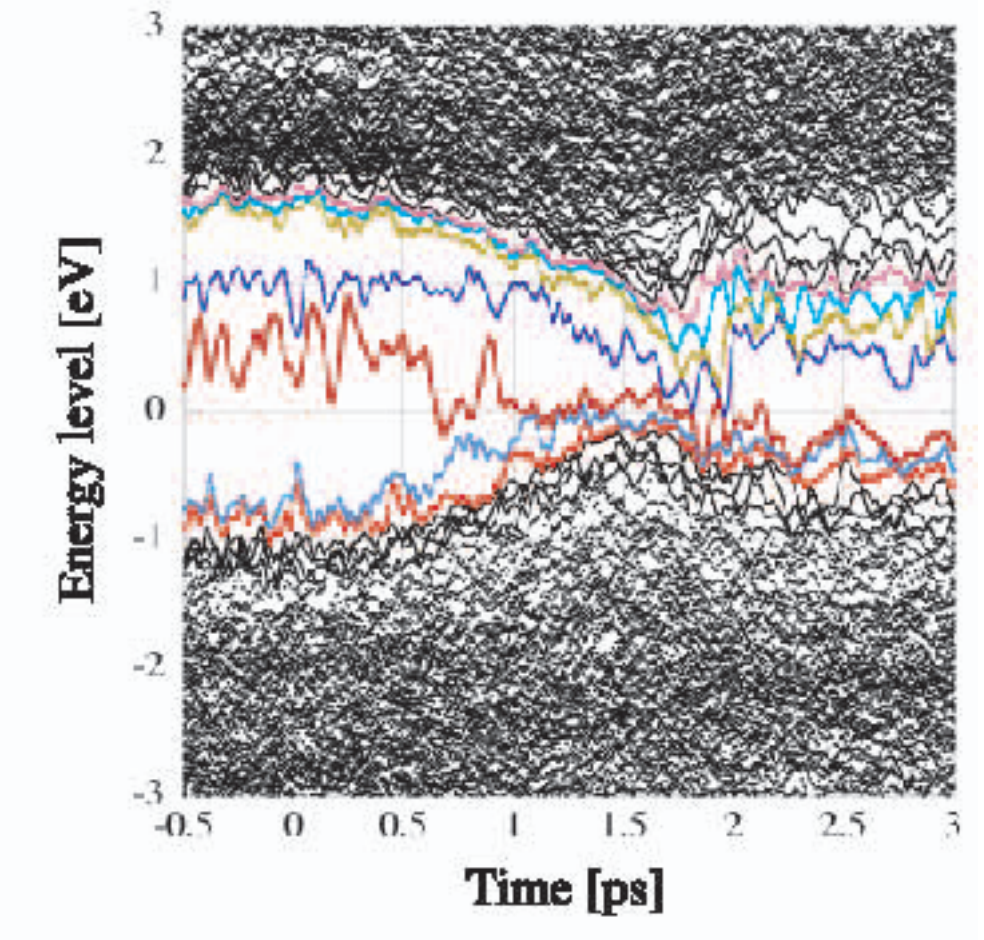

Hoshi and Fujiwara, J. Phys. Soc. Jpn. **72**, 2429 (2003)

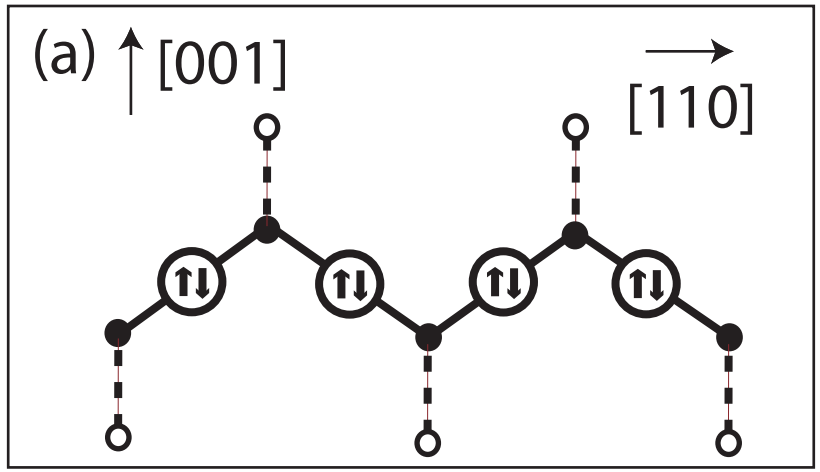

Wannier state in elementary fracture process

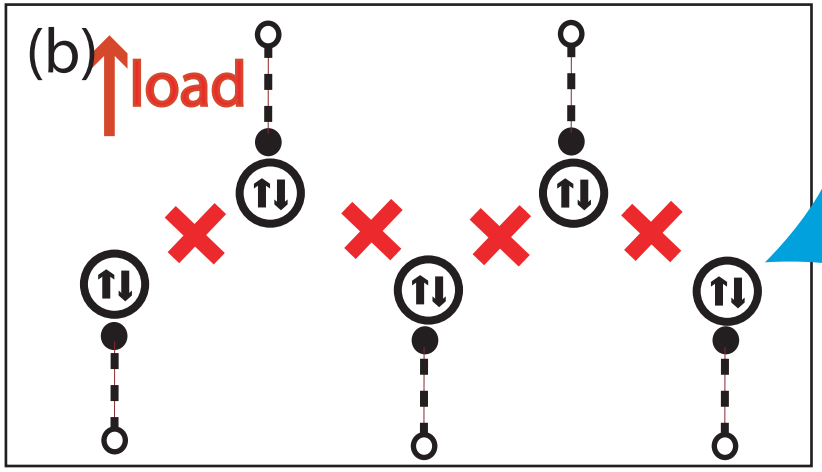

transitional atomic orbital (s-rich)

Time

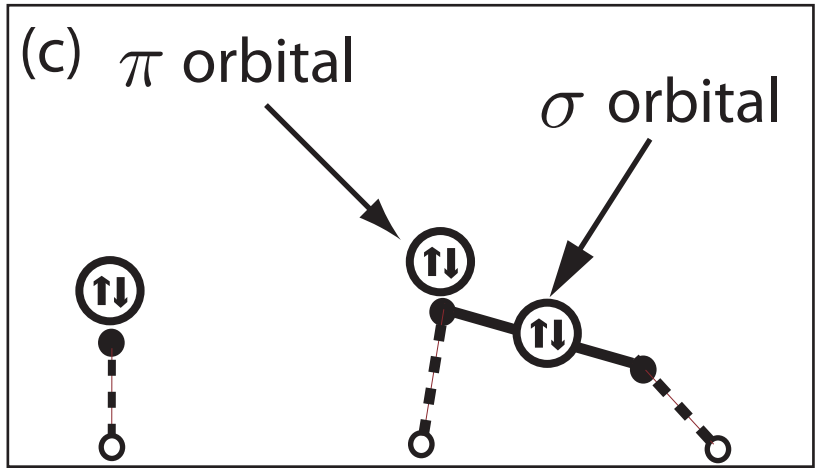

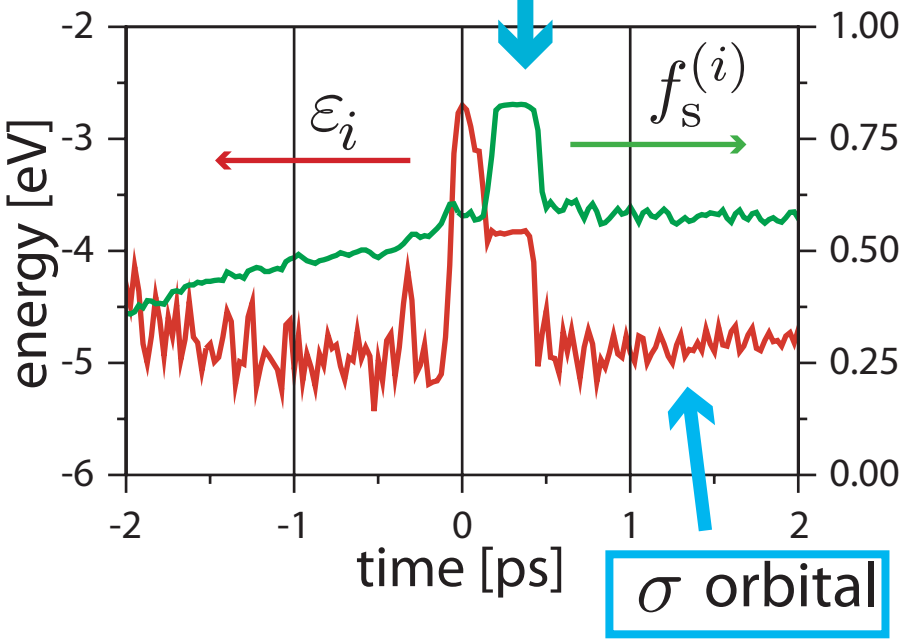

4501 Si (001)

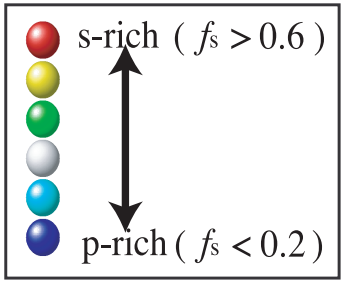

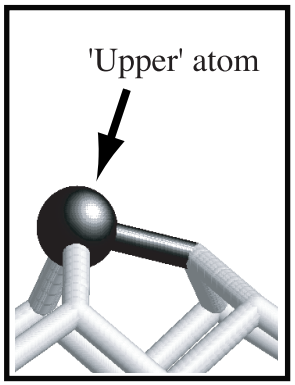

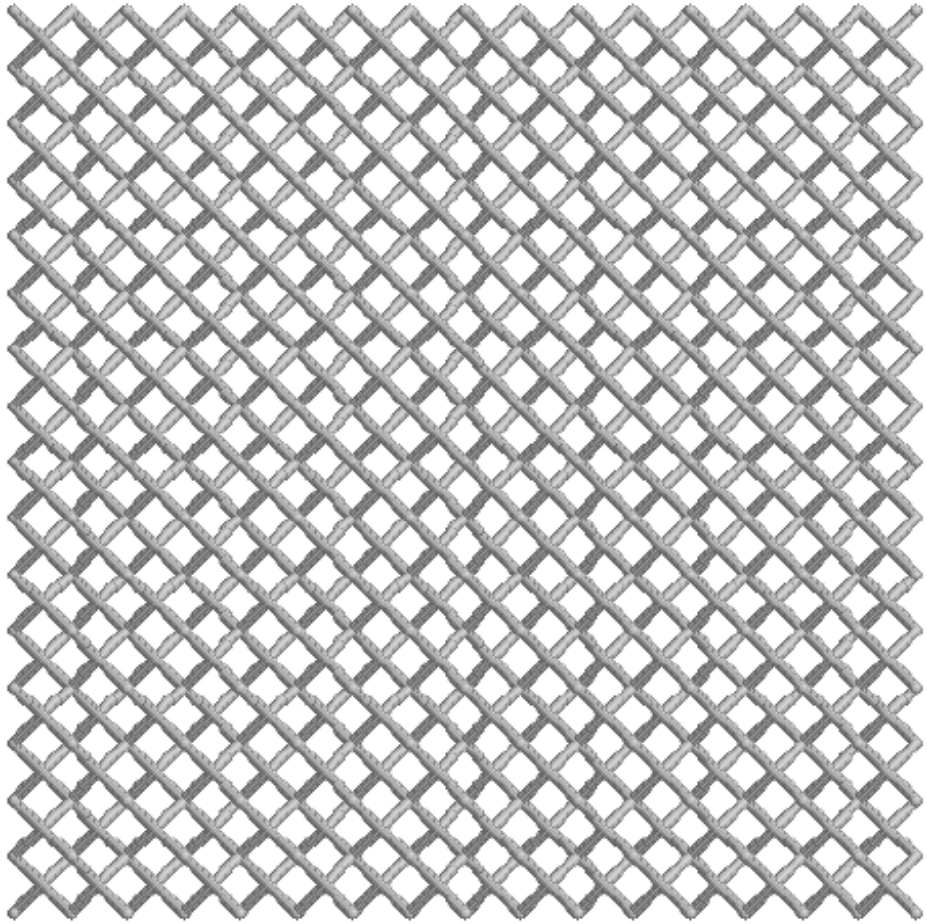

Dynamical fracture simulation in Si(001) surface (4501atoms)

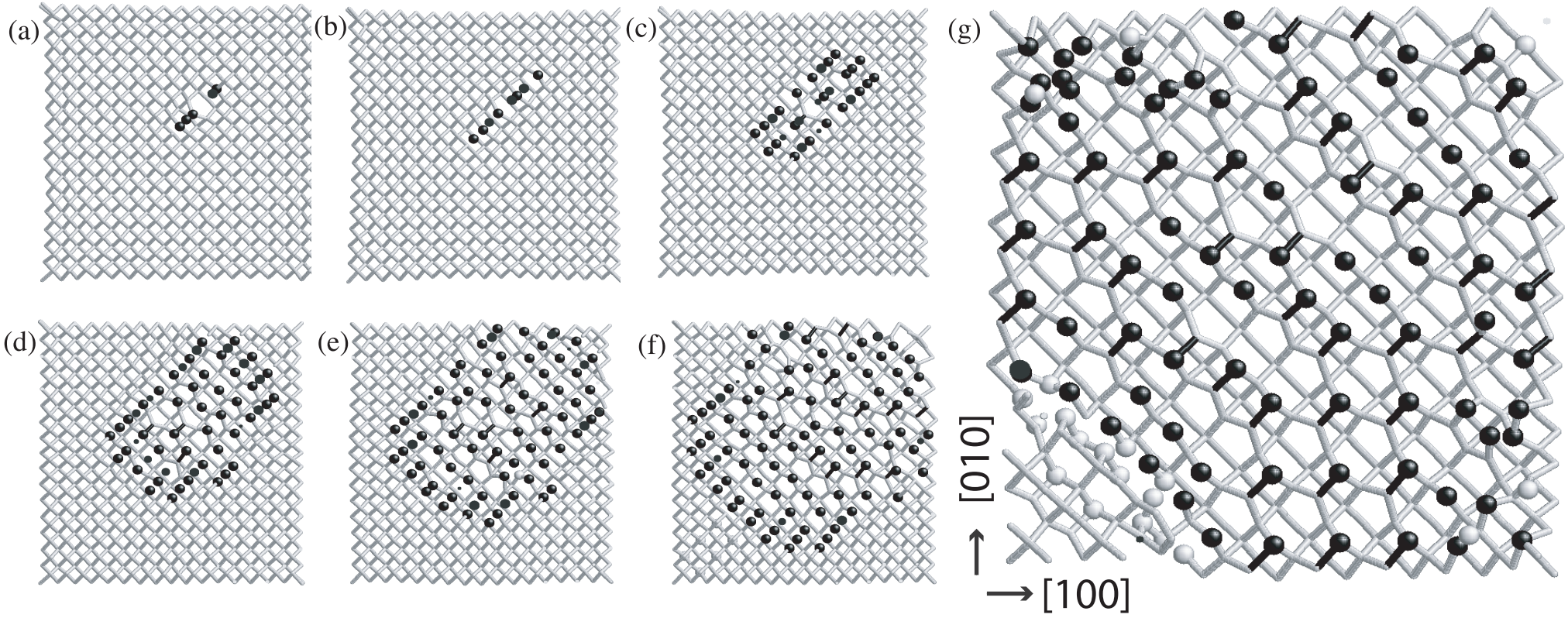

FIG. 2: Snapshots of a fracture process in the (001) plane. The sample size is $n_{100} \times n_{010} \times n_{001} = 33 \times 33 \times 33$ (4501 atoms). The time interval between two successive snapshots is 0.3 ps, except that between (f) and (g) (about 1.3 ps). A set of connected black rod and black ball corresponds to an asymmetric dimer, as in Fig. 1(b) . The left-down area has not yet fractured.

Hoshi and Fujiwara, J. Phys. Soc. Jpn. **72**, 2429 (2003)

Application : Si(111)-(2x1) cleavage simulation

→ π-bonded (Pandey) structure with tilting
Steps are formed in large (10-nm-scale) samples

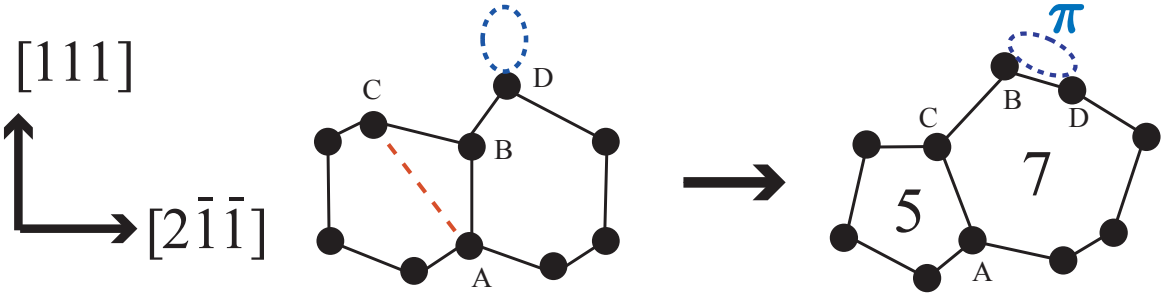

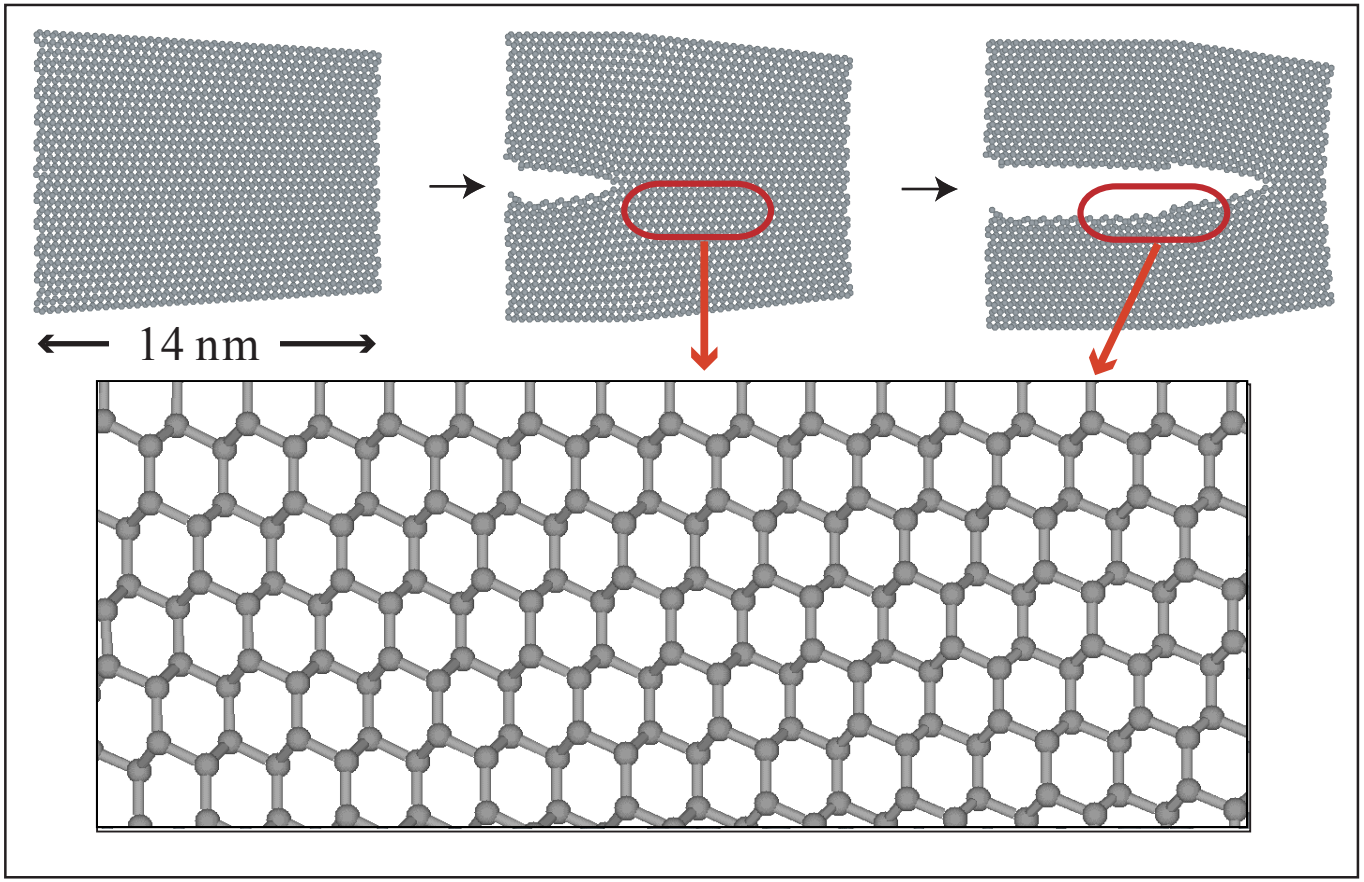

Hoshi, Iguchi and Fujiwara
Phys.Rev. B72, 075323 (2005)

Surface (π-bonding) state

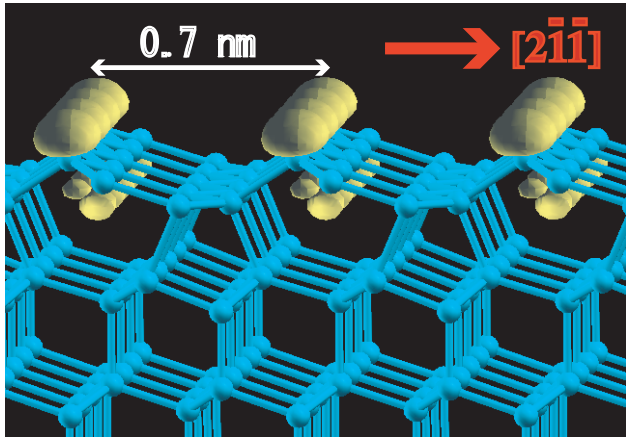

Example of STM experiment

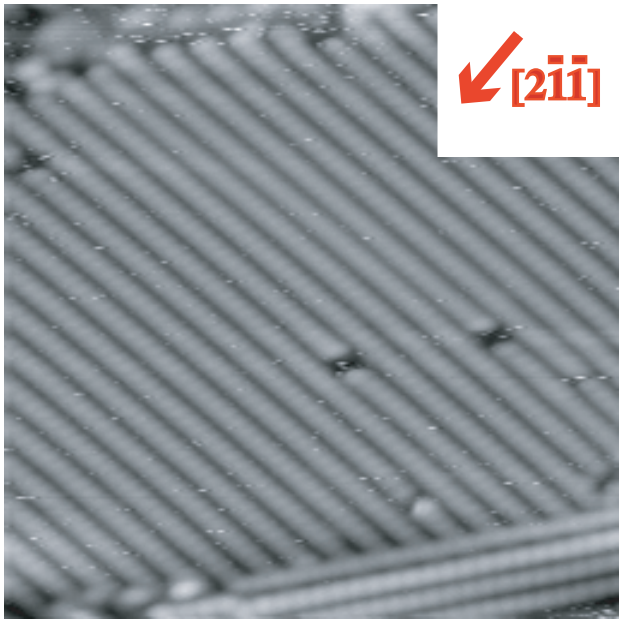

Mera, *et al.*, Ultramicroscopy, (1992)

Application : Si(111)-(2x1) cleavage simulation

→ π-bonded (Pandey) structure with tilting
Steps are formed in large (10-nm-scale) samples

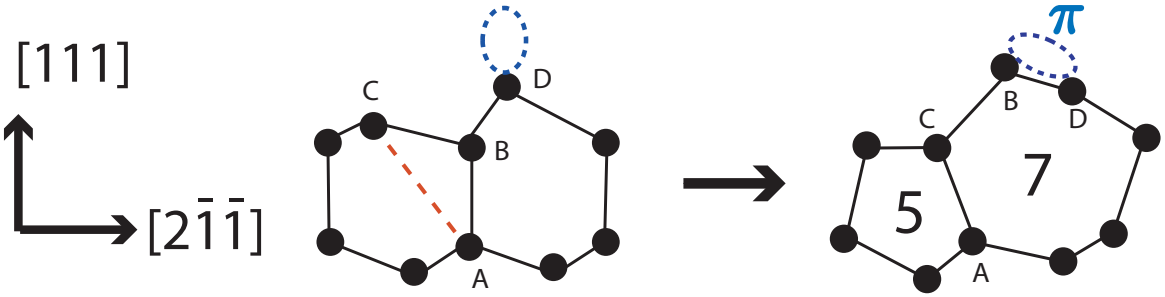

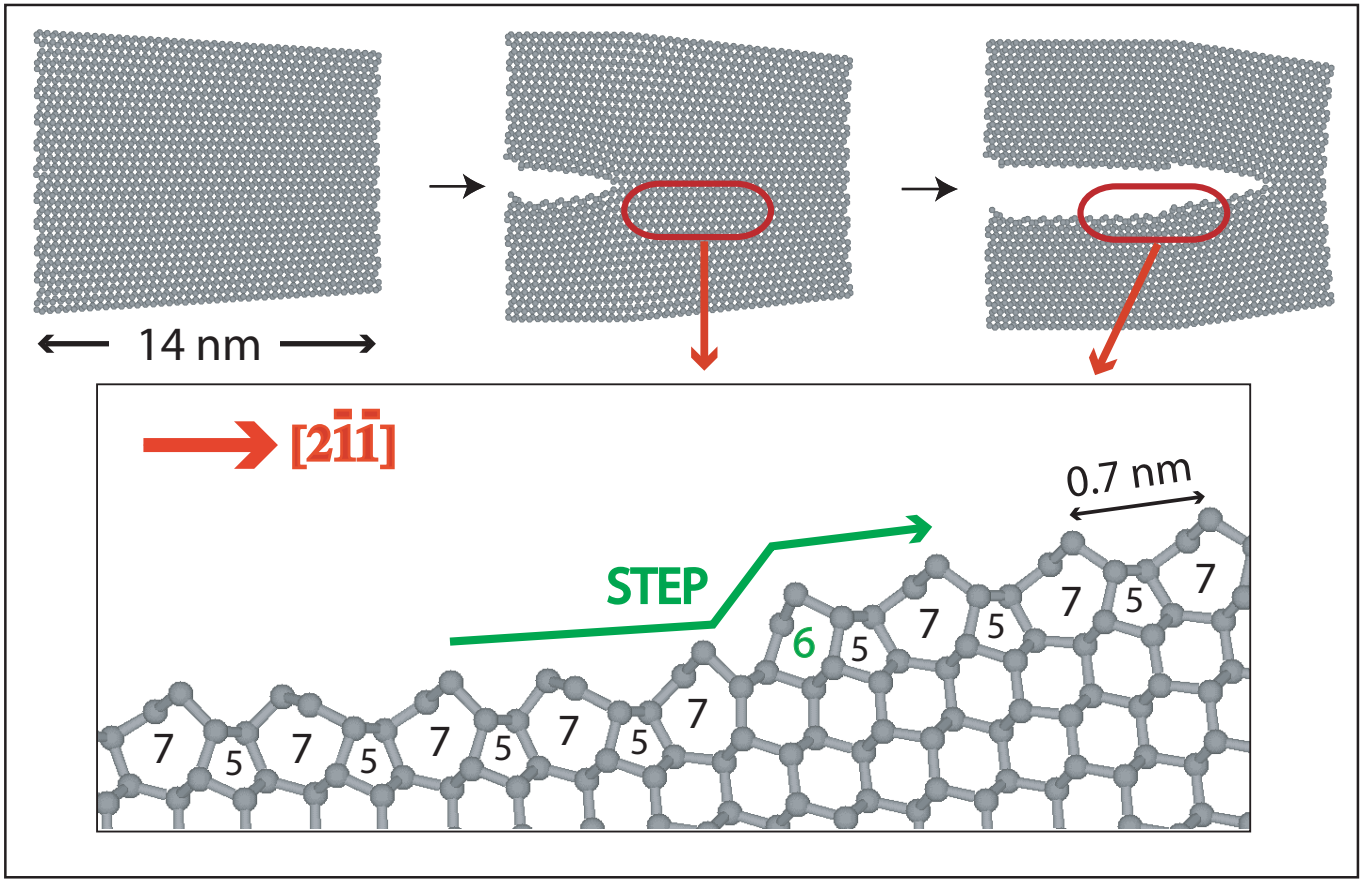

Hoshi, Iguchi and Fujiwara
Phys.Rev. B72, 075323 (2005)

Surface (π-bonding) state

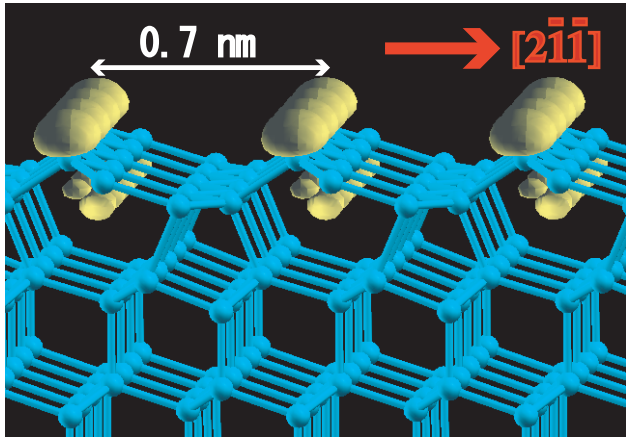

Example of STM experiment

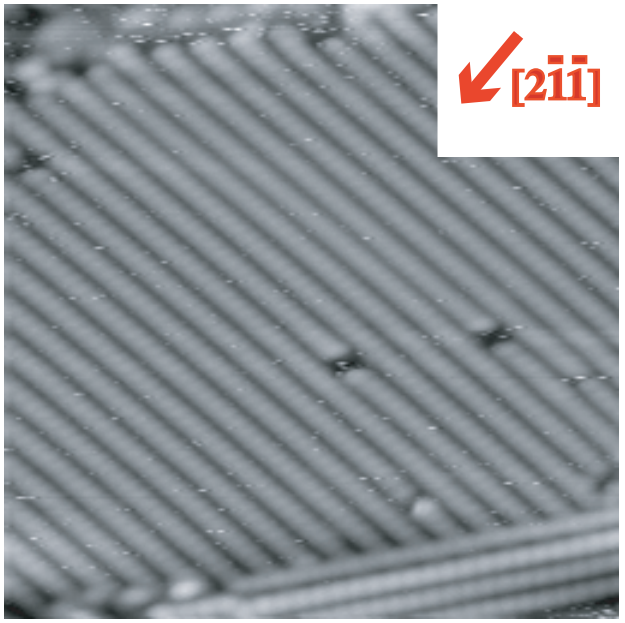

Mera, et al., Ultramicroscopy, (1992)

Quantum mechanical analysis on Si(111) reconstruction process

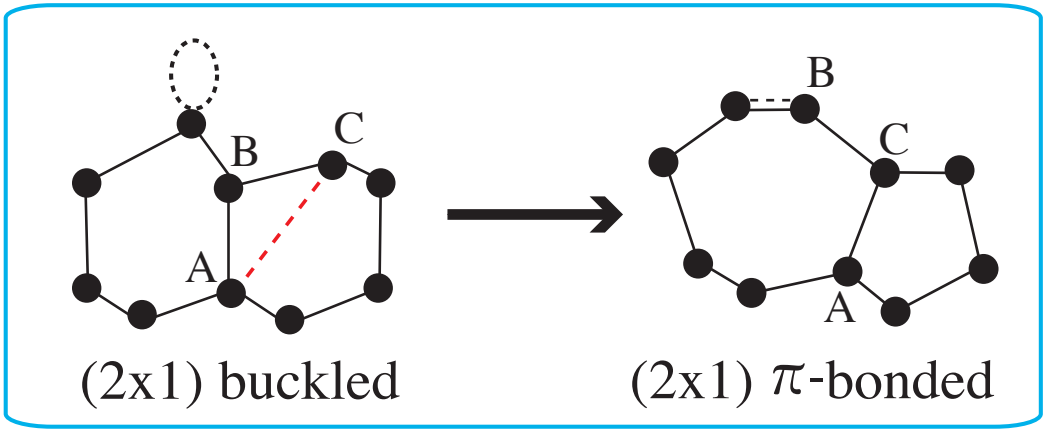

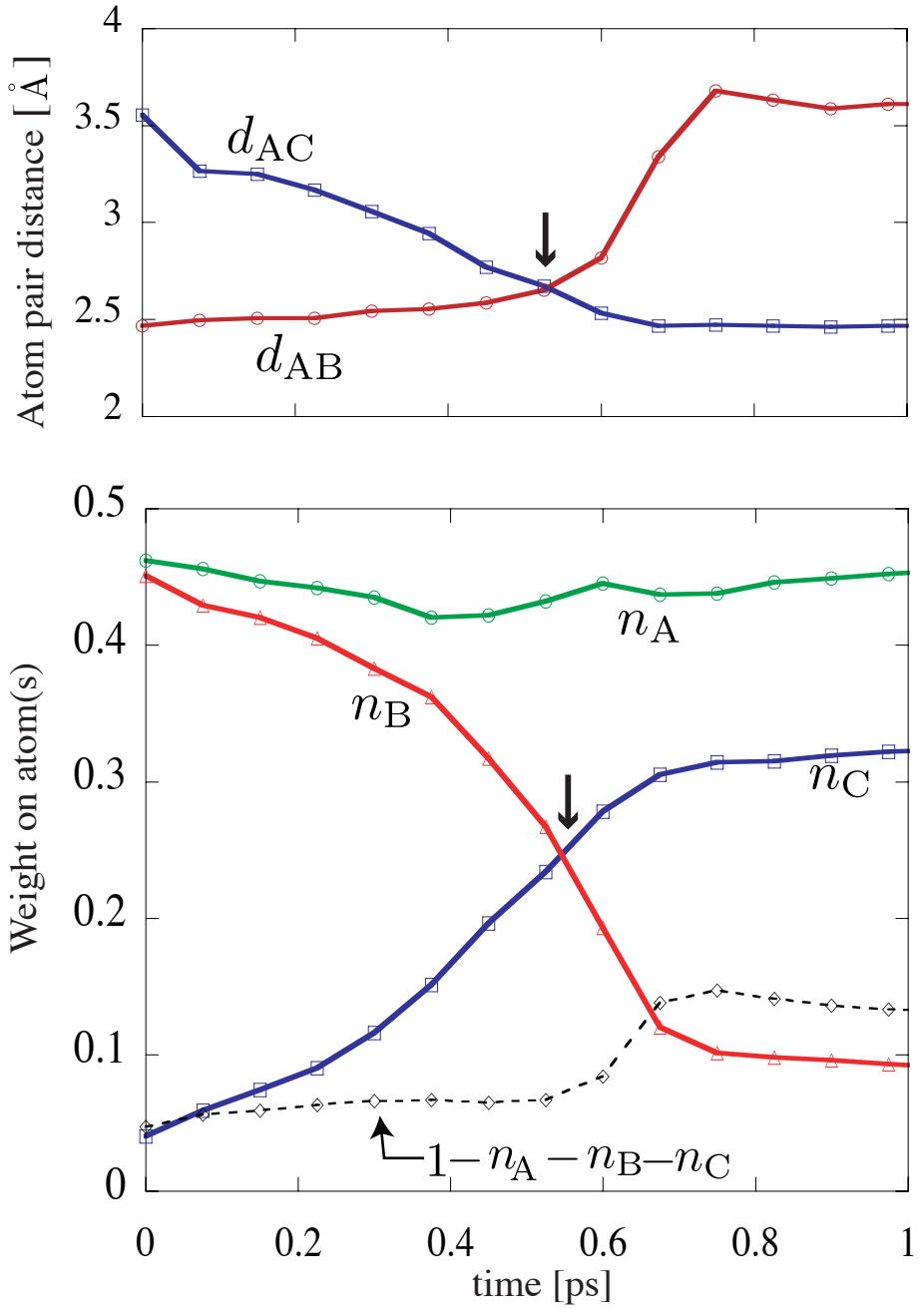

Fig. Quantum mechanical analysisof the wfn.

n_A, n_B, n_C : weights on the atoms

Bending of cleavage path into favorite planes

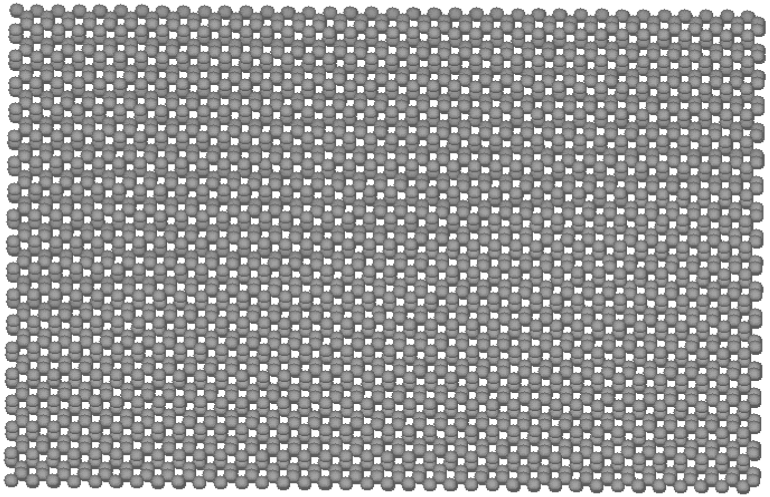

Hoshi, Iguchi and Fujiwara
Phys.Rev. B72, 075323 (2005)

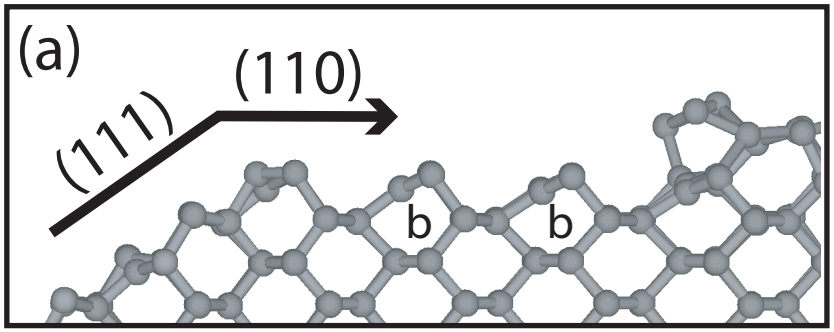

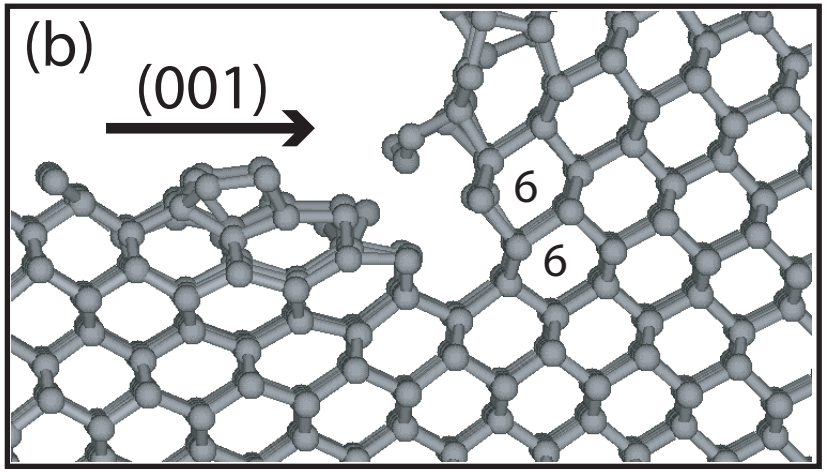

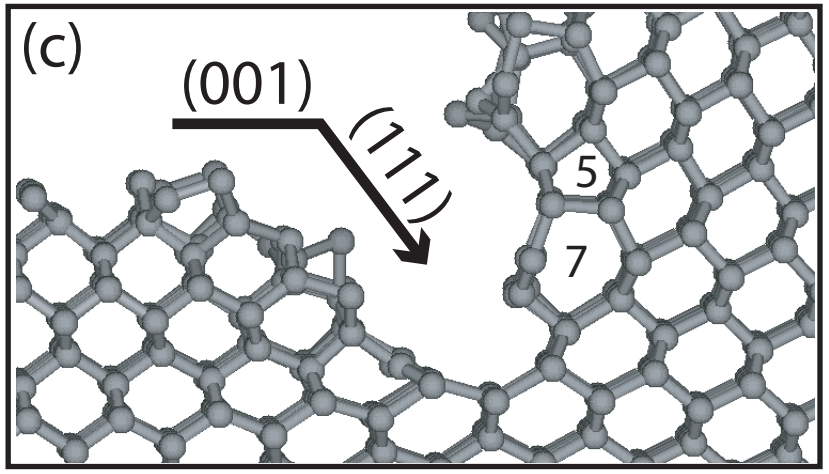

Bending of cleavage path into favorite planes

Hoshi, Iguchi and Fujiwara
Phys.Rev. B72, 075323 (2005)

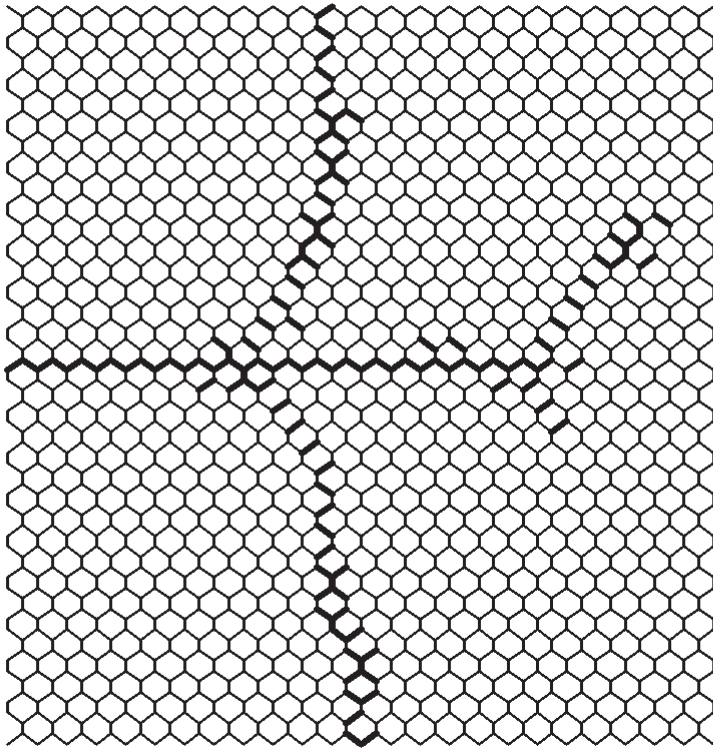

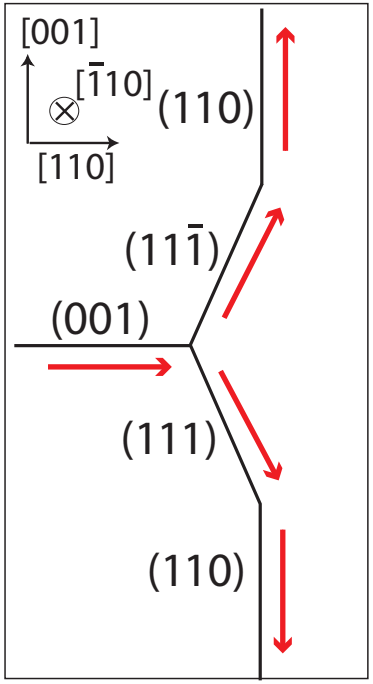

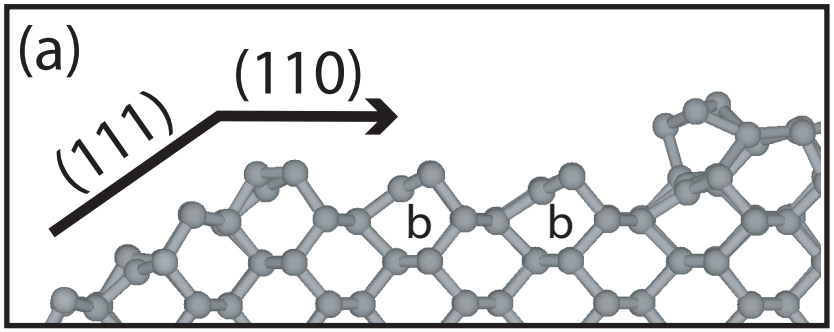

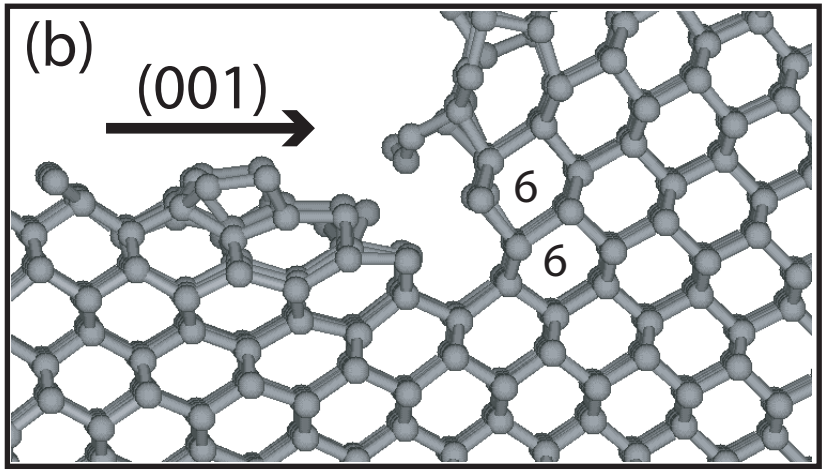

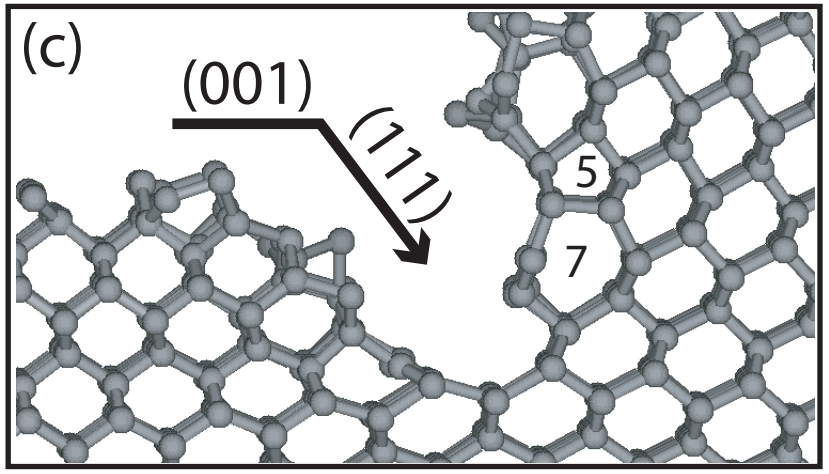

Summary of Si fracture simulation 10^2-10^5 atoms

(001) plane

(1) **Elementary process** for fracture :(2x1)structure
  (a) Two-stage elementary process : dehybridization and charge transfer
  (b) Formation of flat Si(001) surfaces with asymmetric dimers
  (c) Two fracture mechanisms within a single atomic layer
      between the [110] and [1-10] directions

(2) **Anisotropic** behavior and **step** formation

(3) Crossover between nanoscale and macroscale behavior

(111) plane and change of cleavaged plane

(1) **Surface reconstruction** for fracture :(2x1)structure
  Two-stage elementary process
  Charged atom and buckled bonded pair

(2) Step formation through (1-1-1) and (100) planes

Application-2

Fracture Propagation in Si Crystals
Growth Mechanism of Carbon Nanotube
Gold Helical Multishell Nanowire

Zhang, Hoshi and Fujiwara
unpublished

Elongated growth process of SWCNT from liquid carbon

(acceleration test: high density, high temperature)

SWCNT : (9,0)
Density : 1.7 g/cm3
Growth velocity: 30 m/s
Simulation time : 86 ps

Elongated by more than 2nm
Follow structure of wall
Defects

The Nose-Hoover thermostat
is used to control the total
kinetic energy of the system.
(T=4800 K)

The local temperature of
the upper CNT tip is kept
to be lower than that
of the liquid part. (3800K)

Cooling process

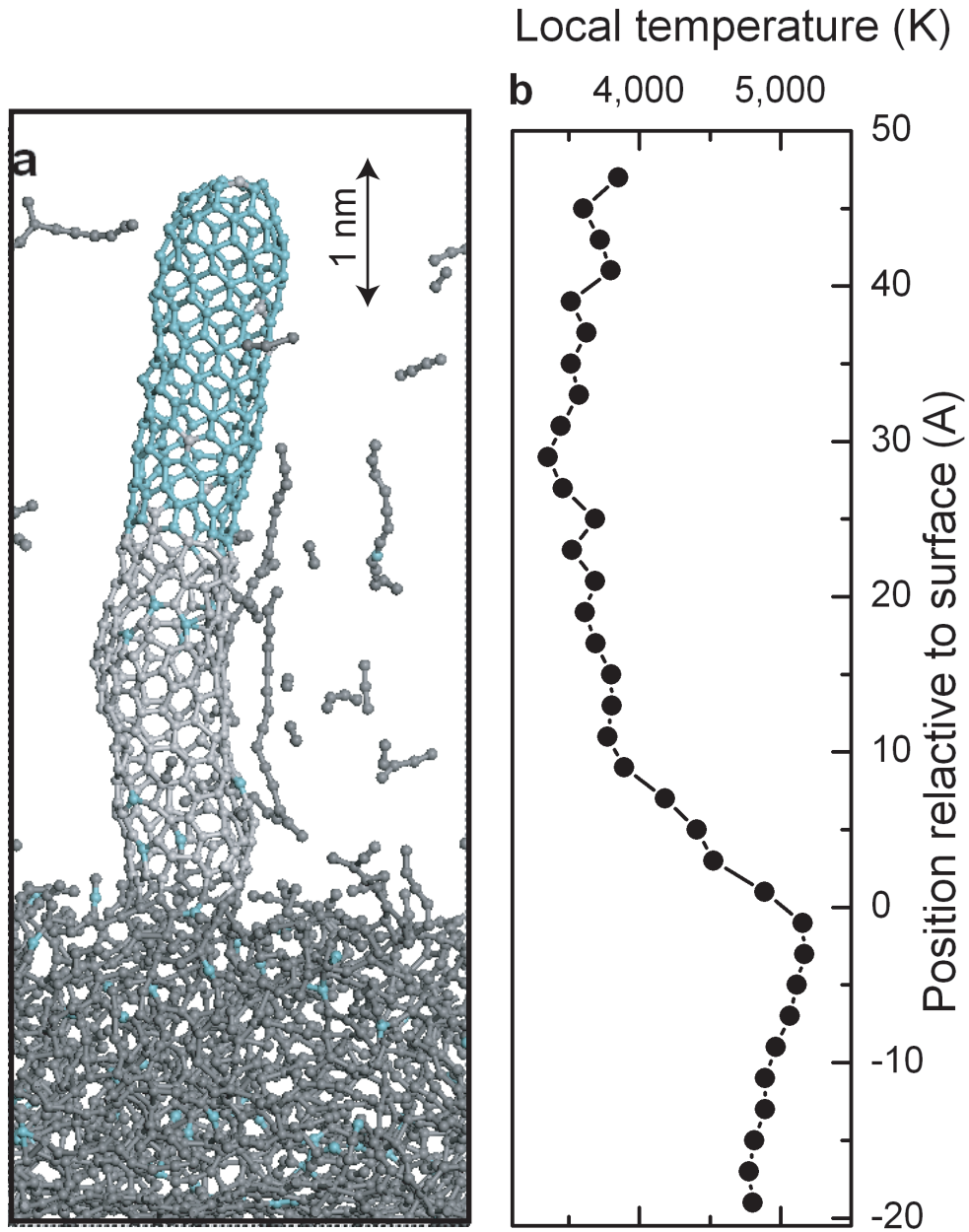

The atoms come into CNT through surface region

Two-fold carbon atoms are majority in surface region

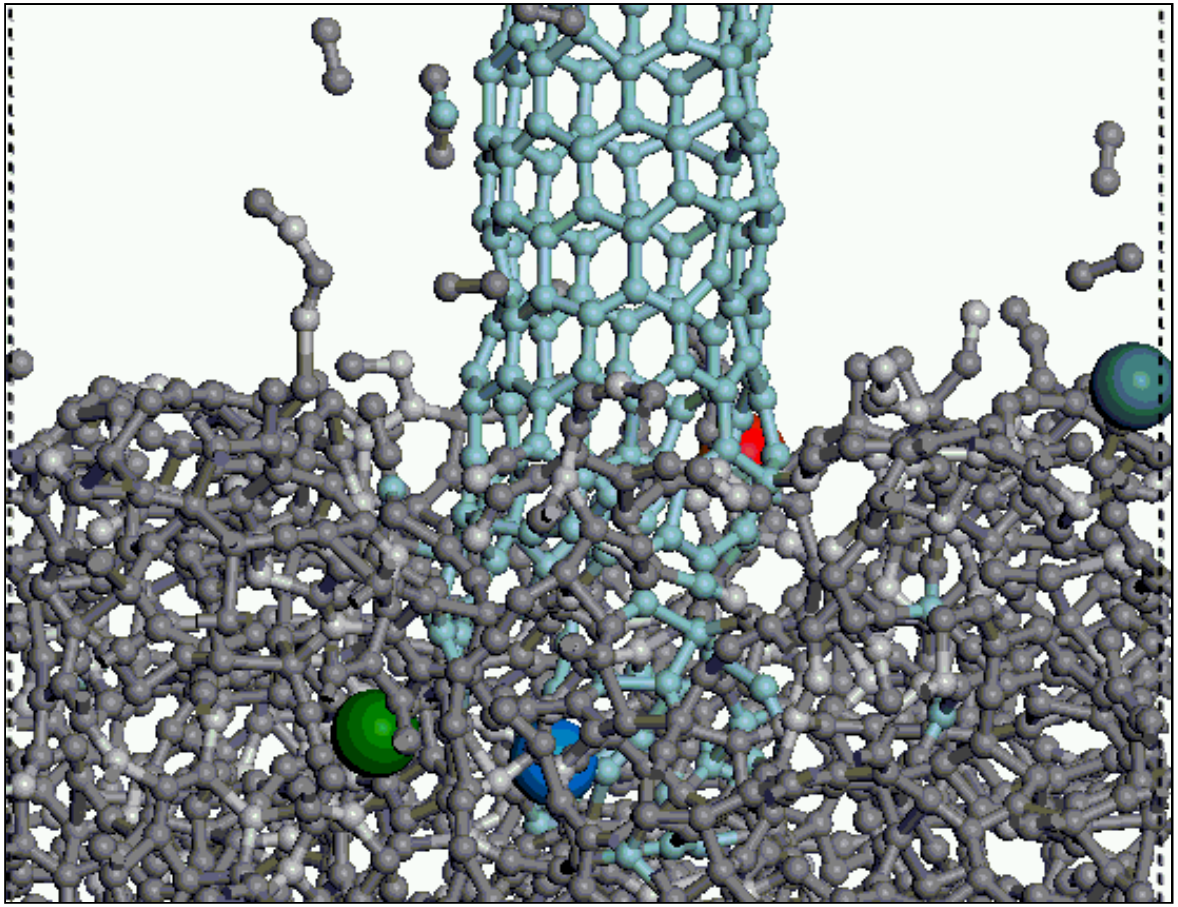

9.0 ps ⟶ 20.1 ps

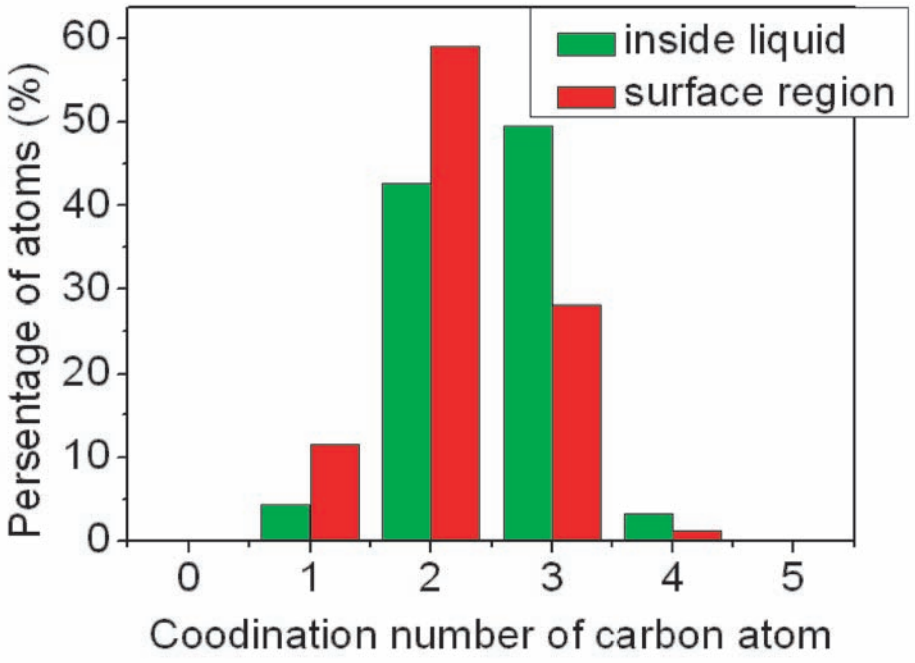

Defect Healing Process

trimer R1-R3 attaches to G1.

tentagon-pentagon -> unstabel decagon

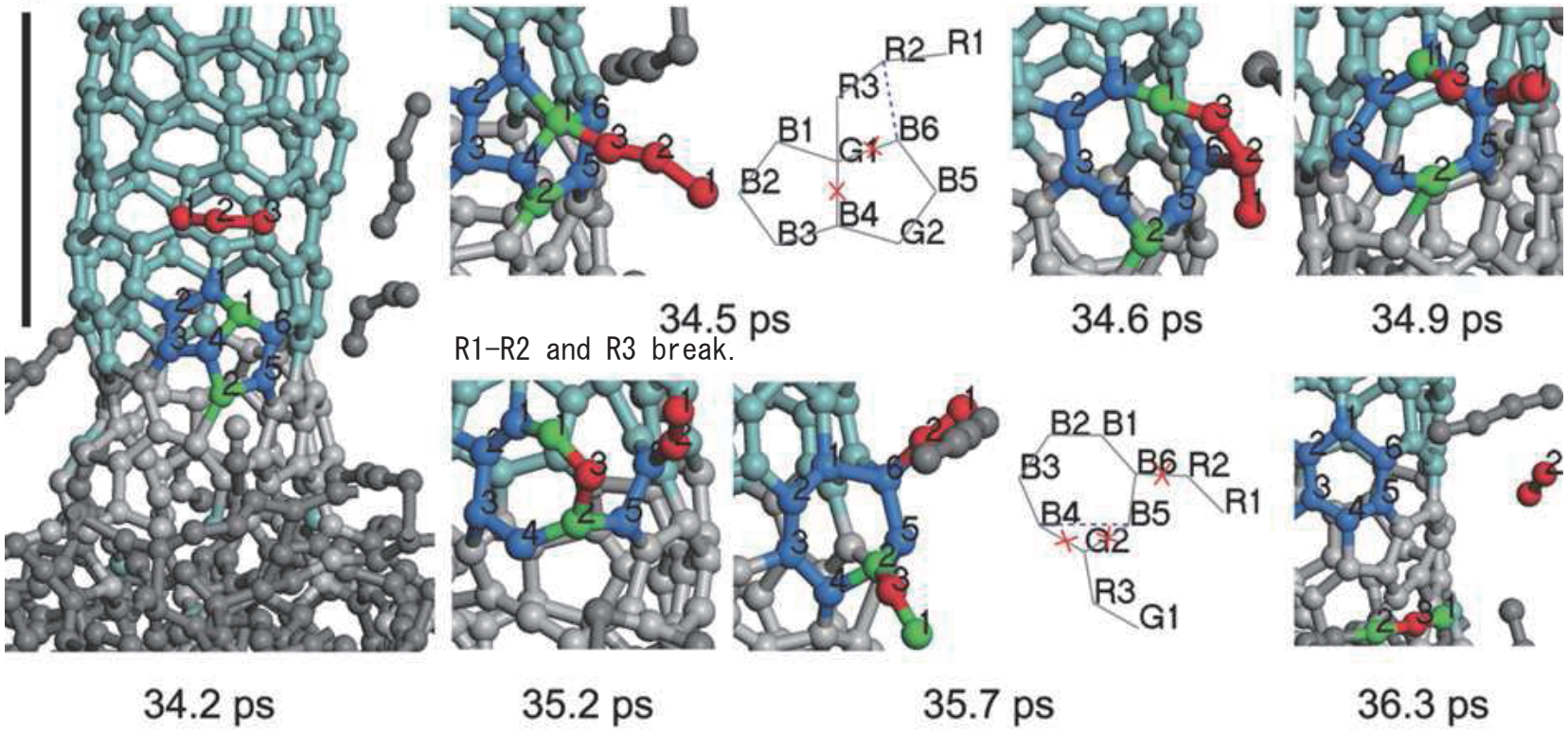

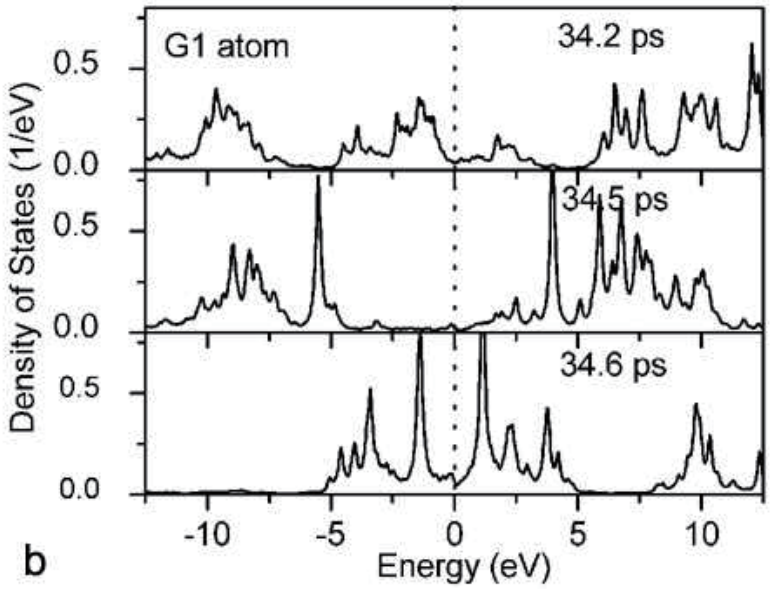

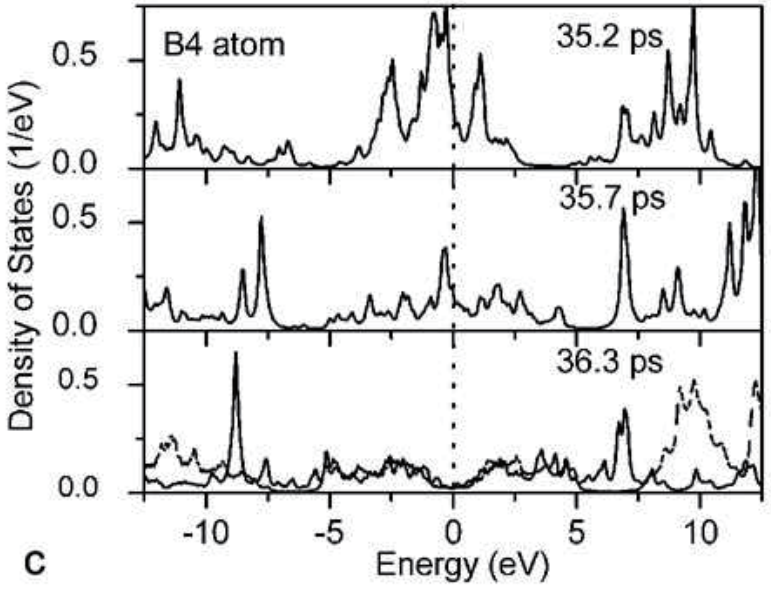

Comparison with the ideal (9,0)CNT

Summary of Simulation for metallic systems
: Growth mechanism of C-nanotube

Large scale Quantum Mechanical Simulation (Krylov subspace)

(1) **Liquid precursor** for growth of C-nanotube
(2) **Linear chain-like structure** in the surface region of liquid C
(3) **Defect healing** process

Applications

Fracture Propagation in Si Crystals
Growth Mechanism of Carbon Nanotube
Gold Helical Multishell Nanowire

Iguchi, Hoshi and Fujiwara,
to be published in PRL

Gold helical multishell nanowires

Magic number, Multi-shell structure, Helicity

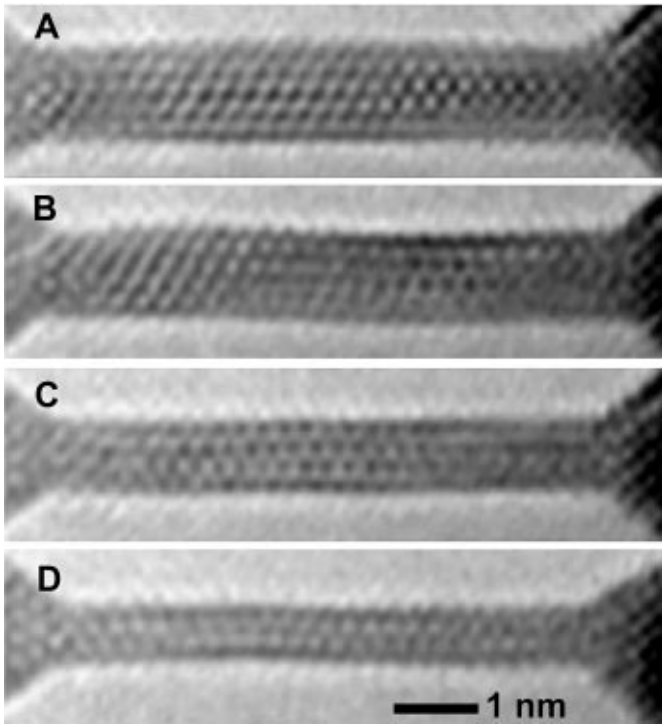

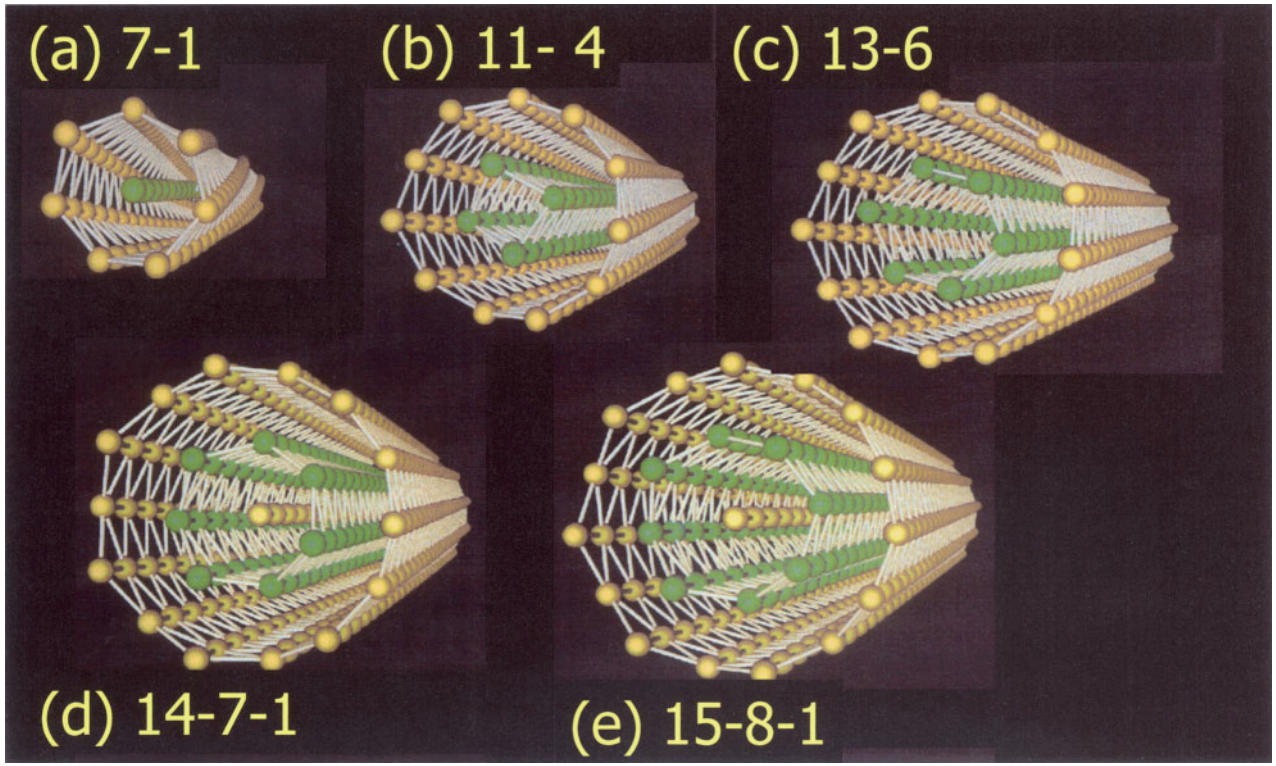

Y.Kondo and K.Takayanagi

Science **289**, 606 (2000)

Y.Ohshima, Y.Kondo and K.Takayanagi,

J. Electron Microscopy, **52,** 49 (2003)

Magic number

Kondo *et al.*, Science **289**, 606 (2000)

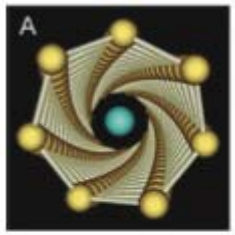

7-1

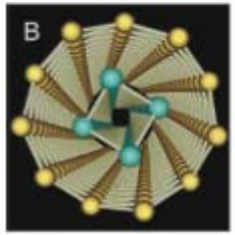

11-4

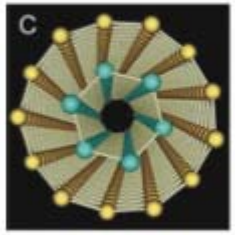

13-6

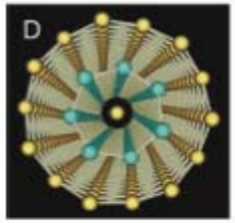

14-7-1

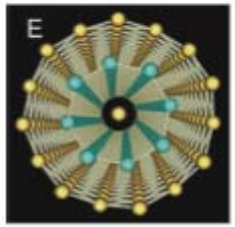

15-8-1

1. Peak structure in appearance frequency

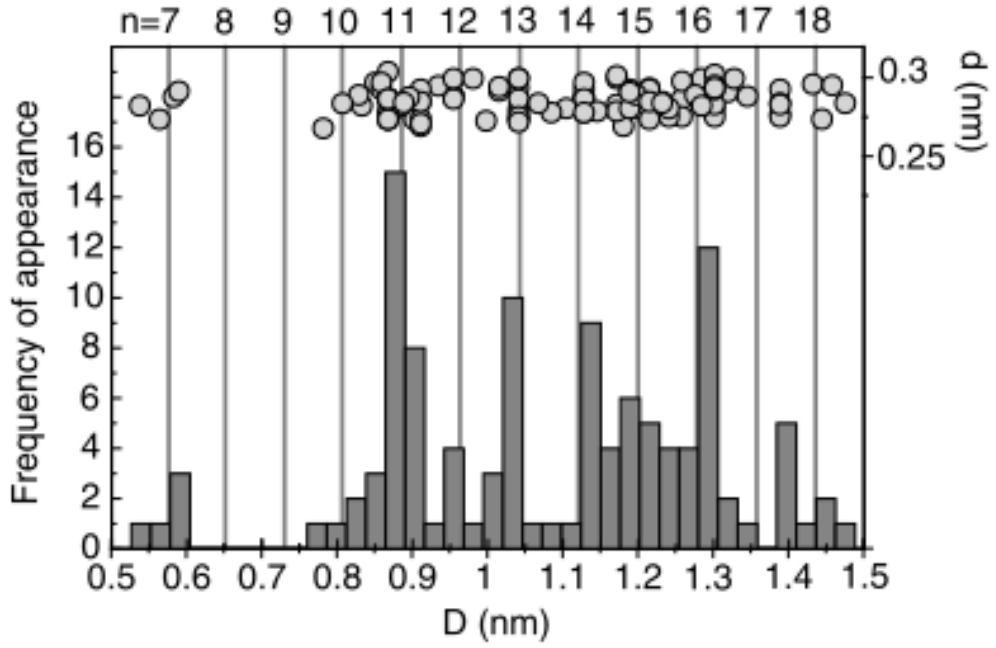

2. Difference of atom numbers between the outermost and next shells is seven.

(Magic number)

Two-stage model for helical multishell nanowire

(a) Ideal multishell structure without helicity

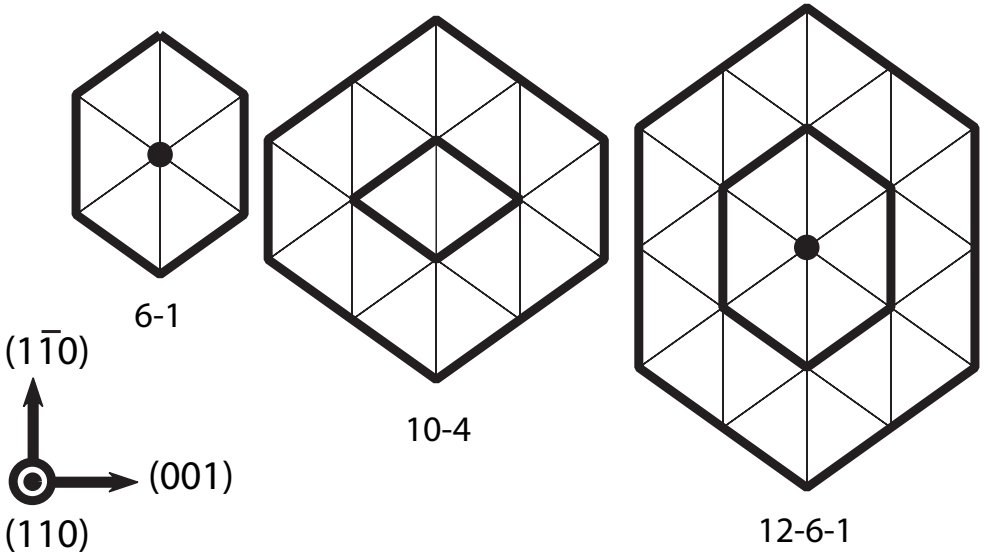

(b) Slip deformation of an atom row

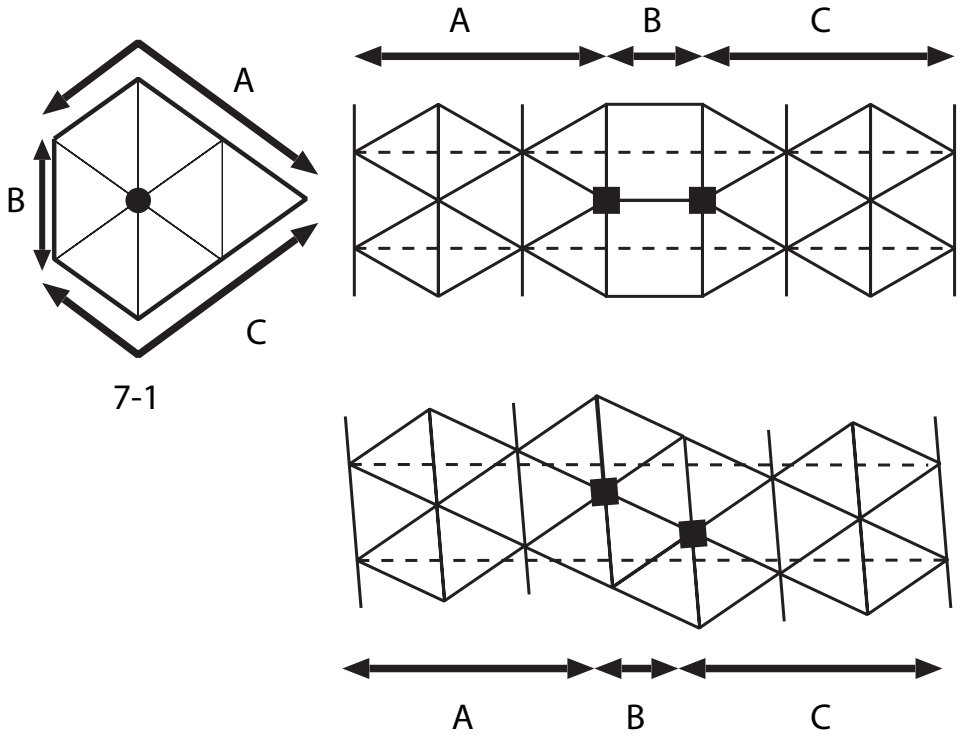

Stage 1: *Dissociation of atoms on the outermost shell from the inner shell*

Stage 2: *Slip deformation to introduce the helicity*

Energy and structure change

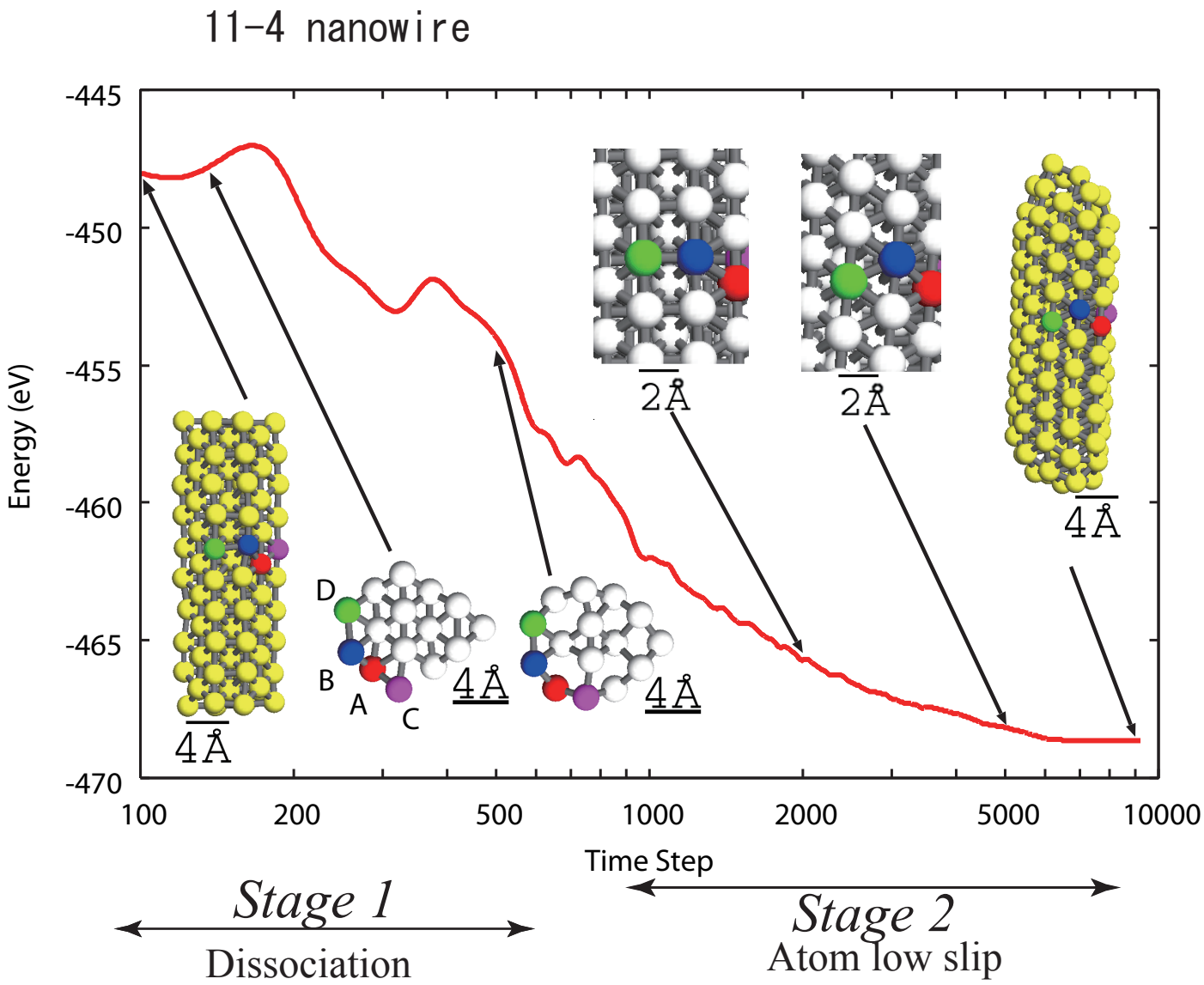

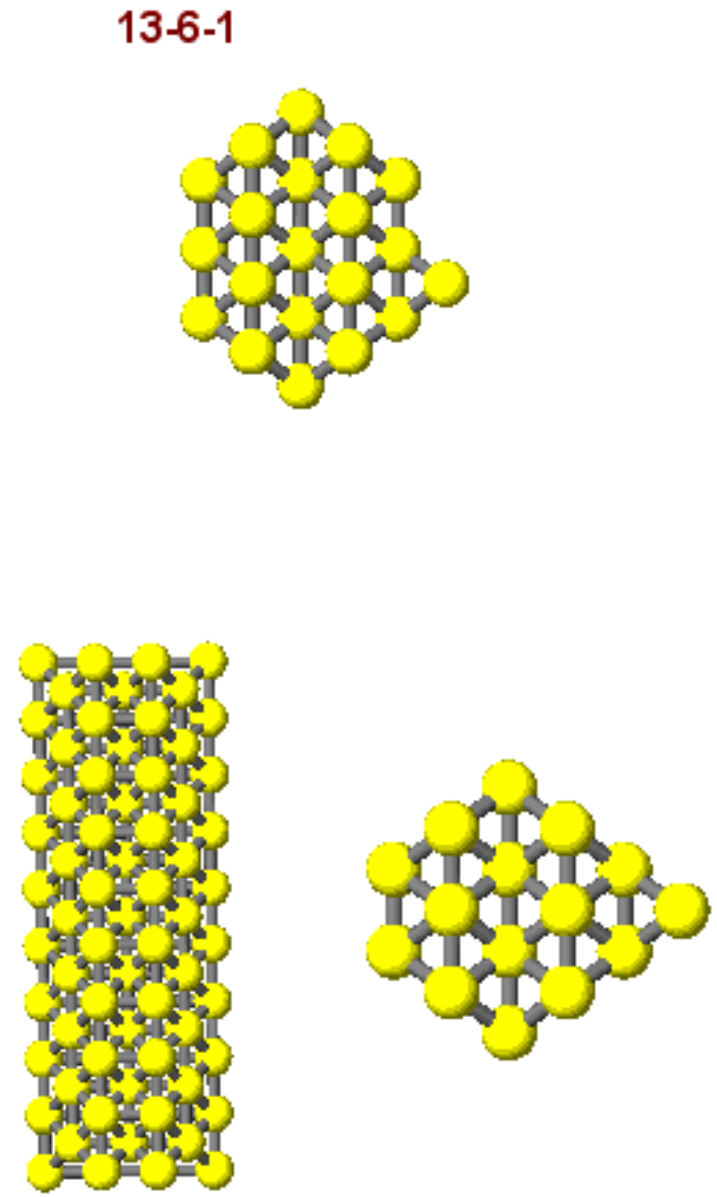

Gold helical multishell nanowires

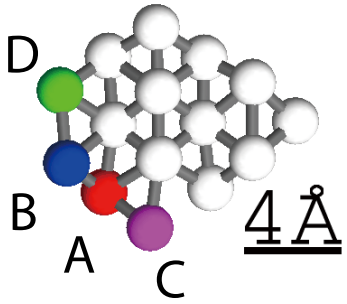

Local Density of States (11-4 Au nanowire)

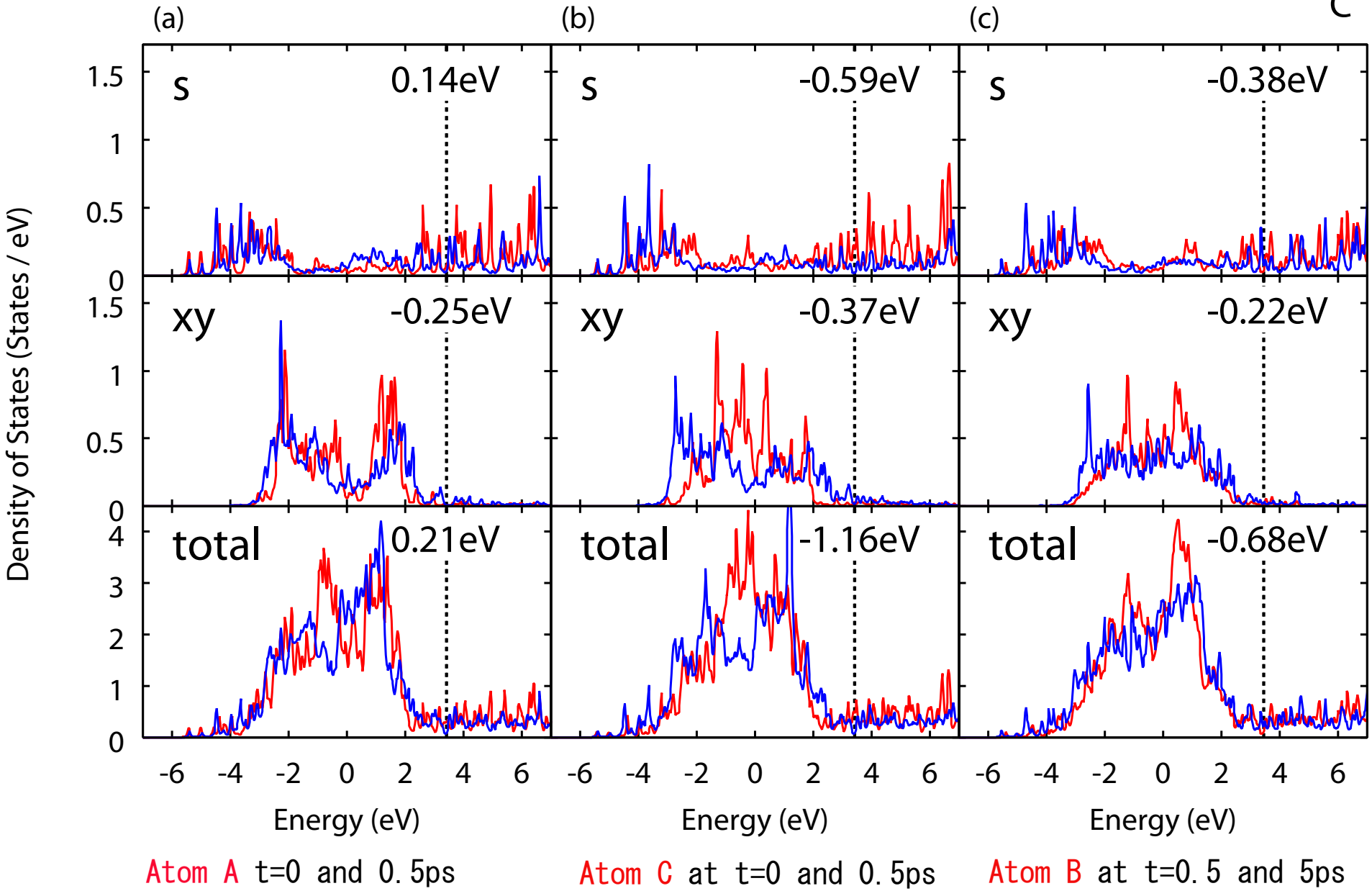

Atom A t=0 and 0.5ps

Atom C at t=0 and 0.5ps

Atom B at t=0.5 and 5ps

Summary of Simulation for metallic systems
: Gold helical multishell nanowire

Two-stage model of gold helical multishell nanowire

(1) Effectivity of NRL Tight-binding Hamiltonian
(2)Nano-science

(1) Two stage model
   a. Dissociation of atoms on the outermost shell from inner one.
   b. **Slip deformation** of atoms row with generating (111) surface.
(2) Competition between s- and d-electrons.
(3) Magic number, helicity, multi-shell structure.

Summary for Method of the Electronic Structures in Large Systems

10^4~10^7 atoms (10~100nm)

Tight-binding formulation of the total electronic energy

Generalized Wannier states --- Unitarity freedom of eigen states

(1) Density matrix represented by Wannier states

(2) **Insulators / semiconductors**

Krylov Subspace Method

Subspace diagonalization method

Shifted COCG method

(1) Density matrix in Krylov subspace

(2) **Insulators / semiconductors and metals**

Hybrid scheme by dividing the Hilbert space

Prallelization

Original method and Program-Code

Problems in future
: Preparation for Hamiltonian

Tight binding Hamiltonian
** Possibly Outer Loop of LDA Hamiltonian*

(1) Empirical TB Hamiltonian :

[Si, Ge, C: sp^3 model] Kwon et al., Phys. Rev. B **49**, 7242 (1994). cf. sp^3s^* model

(2) Non-orthogonal TB Hamiltonian (NRL):

[Au, Cu, wide range of elements]

M. J. Mehl and D. A. Papaconstantpoulos, Phys. Rev. B **54**, 4519 (1996),
F. Kirchhoff et al., Phys. Rev. B **63**, 195101 (2001).

(3) Orthogonal/Non-orthogonal TB Hamiltonian with repulsive potentials

Xu et al., J. Phys. Cond. Matt. **4**, 6047 (1992).

Bond-order potential with repulsive potentials

Mrovec et al., Phys. Rev. B **69**, 094115 (2004).

(4) Gaussian or atomic orbital base (Gas phase parameters)